



## Neotectonics of the volcanic Kuei-Shan Tao island, and geodynamic implications (NE Taiwan - SW Okinawa Trough)

Benoit Deffontaines<sup>a,b</sup>, Kuo-Jen Chang<sup>a,c,\*</sup>, Pichun Huang<sup>d</sup>, Ho-Han Hsu<sup>a,e</sup>, Shu-Kun Hsu<sup>a,d</sup>, Char-Shine Liu<sup>a,e</sup>, Chyi-Tyi Lee<sup>a,f</sup>, Samuel Magalhaes<sup>g</sup>, Gérardo Fortunato<sup>g</sup>

<sup>a</sup> International Research Project « From Geodynamic to Extreme Events » G2E, CNRS-MOST France, Taiwan

<sup>b</sup> Laboratoire de Géomatériaux et Géologie de l'Ingénieur (G2I), Ministère de l'Enseignement Supérieur, de la Recherche et de l'Innovation, & Université Marne-La-Vallée, F-77454 Marne-la-Vallée, France

<sup>c</sup> Department of Civil Engineering, National Taipei University of Technology, Taipei 10654, Taiwan, ROC

<sup>d</sup> Department of Earth Sciences, National Central University, Taiwan, ROC

<sup>e</sup> Institute of Oceanography, National Taiwan University, Taipei, Taiwan, ROC

<sup>f</sup> Graduate Institute of Applied Geology, National Central University, Chungli, Taiwan, ROC

<sup>g</sup> Alphasigma SAS, 62, rue du Cardinal Lemoine, 75005 Paris, France

### ARTICLE INFO

#### Keywords:

Neotectonics  
Unmanned Aircraft System (UAS)  
Digital Surface Model (DSM)  
Geological mapping  
Volcano  
Landslide  
Geodynamics  
Kuei-Shan Tao  
South-West Okinawa Trough  
North-East Taiwan

### ABSTRACT

What are the geodynamic processes during the transition from the onshore NE Taiwan collision to the offshore southwest Okinawa back-arc basin opening associated to the Ryu-Kyu subduction? What is the local neotectonic scheme of this transition (e.g.: structural sketch map of the outcropping volcanic edifice highlighting major faults and their associated earthquakes)? These are some of the fundamental questions addressed to the Kuei-Shan Tao volcanic island (KST hereafter) which is the unique emerged volcanic outcrops situated within this geodynamic transition area.

Several incompatible KST geological mappings had been published without any faults, nor dykes, nor feeders (Ichikawa, 1934; Hsu, 1963; and Chiu et al., 2010) that needed to be updated and completed on the structural point of view. In order to do so, we acquired a new high resolution UAS-drone topography (Digital Surface Model) through photogrammetric processing, with a ground resolution <10 cm. We analyse and interpret it in detail using morphostructural photo-interpretation methods. Field works on KST is restricted due to technical and administrative reasons, so we compare our morphostructural map to the shoreline outcrops observed from a boat survey. Then, we have updated the Kuei-Shan Tao geological mapping (lava flows and pyroclastic falls), and the structural scheme as well as the major erosion landslides processes. Taking into account the re-interpretation of surroundings offshore bathymetry, old and new seismic profiles, the different drillings done in the Kuei-Chia northern flank, previous geophysical works, the existing massive andesite datings), as well as the inferred stress regimes deduced from the earthquake's focal mechanisms, we propose a KST neotectonic map. We propose also a new scenario for the recent KST volcanic evolution. Kuei-Shan Tao geology and geodynamics may have a so great importance for the 0.5 millions citizens of the so close flat lying Ilan Plain in terms of natural hazards (eruptions, tsunamis, earthquakes...).

### 1. Introduction

Among the geodynamic problems that remains unsolved in Taiwan, there is the tectonic processes that brings the NE Taiwan plate tectonic collision to the opening of the SW Okinawa trough (SWOT below) which correspond to the back-arc basin associated to the RyuKyu/Okinawa subduction.

Kuei-Shan Tao volcanic island (KST hereafter) is the unique outcrop within this transition area situated in between both the onshore Taiwan collision (Ho, 1986; Teng, 1996; Hsu et al., 1996a, 1996b, Hsu et al., 1998, 2001; Wu et al., 1997, 2009; Kao et al., 1998; Lallemand and Liu, 1998; Shyu et al., 2005; Clift et al., 2008; Angelier et al., 2008...) and the offshore Okinawa back-arc extensive basin (Letouzey and Kimura, 1986; Sibuet et al., 1987, 1995, 1998; Hsu et al., 1996b; up to Tsai et al., 2021).

\* Corresponding author at: Department of Civil Engineering, National Taipei University of Technology, Taipei 10654, Taiwan, ROC.

E-mail addresses: [benoit.deffontaines@univ-mlv.fr](mailto:benoit.deffontaines@univ-mlv.fr) (B. Deffontaines), [epidote@ntut.edu.tw](mailto:epidote@ntut.edu.tw) (K.-J. Chang).

<https://doi.org/10.1016/j.tecto.2022.229362>

Received 9 April 2021; Received in revised form 18 March 2022; Accepted 28 March 2022

Available online 19 April 2022

0040-1951/© 2022 Elsevier B.V. All rights reserved.

Kuei-Shan Tao (surface 2.7 km<sup>2</sup>) is situated offshore the northeastern Taiwan Ilan Plain ( $\approx 10$  km). It is a small calc-alkaline andesitic volcanic island located also at the western tip of the southwest Okinawa Trough (Fig. 1). But we noticed that previous KST geological mappings lack of any faults, dips and structures. Our aim herein is to precise and provide the KST structural schemes and the neotectonic map and their geodynamic implications.

One may note that volcanic areas in the world are often difficult to study from the geological and structural point of views due to their heterogeneity. For instance, lava flows of each eruption may cover only locally contrasting to pyroclastic falls that cover large surrounding areas. Volcanic topographies are then regularly « smoothed » and « renewed » during each eruption and consequently the previous geological features (deposits as well as their deformation) are masked, buried and hidden. Then thicknesses of any volcanic deposits might change abruptly (increase or decrease) locally quickly as they depend on the previous topography. Effectively, as lava flow from top to bottom following the steepest slope and settle in the lower part of the volcanic edifice topography (e.g. former drainage) that lead sometimes to complex mapping geometries. From the structural point of view, lava flows are quite complexe areas to study as cool joints may interfere with tectonic joints. As an example, brecciated areas situated beneath and laterally of the lava flows are almost impossible to access and to study. Moreover, the unconsolidated soft pyroclastic falls do not preserve fault planes nor slickenlines. Massive lava flows also do not register easily slickenlines. Sometimes and seldom oriented mineralisations highlight the deformation and reveal the relative motions on fault planes if the faulting is associated with fluids circulation (Dauteuil and Bergerat, 2005, and pers. comm.). In general, relative motions and displacements are difficult to infer in a volcanic environment, except in the case of vertical offsets revealed by the different displacements of the alternance of lava and pyroclastic fall on both sides of the fault. Consequently, any structural studies in volcanic environments are quite difficult to handle. Deciphering the structures in a volcanic environment is like a complexe puzzle to solve.

In this manuscript, we will look for the structures (dips, faults, providing arguments) to supply an updated geological mapping and propose a neotectonic map that have geodynamic implications.

So, we first focus on the KST geology and published geological mappings. The latter settle the lithologies which are described and re-analysed thanks to two drills situated on the northern flank of Kuei-

Chia in order to precise locally the sequence of the volcanic layers. Then, we acquired a high resolution UAS photogrammetric survey that cover the whole island which enable us to get the KST digital Surface Model (DSM) with a 7.5 cm ground resolution. With morphostructural methods we updated previous geological mapping adding fractures and landslides that affect the volcanic Kuei-Chia and Kuei-Shou volcanic edifices. In addition, an oceanic research survey give us the chance to monitor from the boat the KST shoreline cliffs geology highlighting lithologies as well as some structures. Many fault zones were then evidenced that lead us to update the previous geological mapping. Finally, we were able to propose a scenario for the progressive edification and dismantling of KST island. We conclude by the importance of the monitoring of such volcanic island so close to the Ilan Plain and the Taipei city.

## 2. Kuei-Shan Tao geography and geology

Kuei-Shan Tao so called « Sea turtle » due to its morphology, is composed of (1) Kuei-Shou (« turtle-head », 200 m high) an eroded volcanic fall deposits edifice situated at its eastern tip; (2) Kuei-Chia (« turtle-shell », 401 m high) the main volcanic edifice situated in the central part of the island; in between both Kuei-Chia and Kuei-Shou there is the pass also called « turtle-neck ». The Kuei-Wei (« turtle-tail »), situated at its western tip, is an elongated gravel bar/ridge WNW trending which is 1 km long, 50 m large, 4 to 5 m high; It is closely linked with the sedimentation linked to the Kuroshio Sea currents.

### 2.1. Geology

From the petrographic point of view, lava flows, agglomerates or pyroclastic flows and xenoliths of Kuei-Chia are described below respectively (see Hsu, 1963; Chiu et al., 2010).

- The andesite lava flows are preponderant in amount. Porphyritic they belong to dark two-pyroxene andesite invariably with white plagioclases phenocrystals (hypersthene and augite), sometimes with olivine. Unweathered facies are dense, bluish to grayish in colour contrasting to the weathered facies more porous, reddish to brownish in colour as the phenocrysts are rimmed with reddish iron ore. The latter is weathered, get easily pulverized under fingers and is easy to

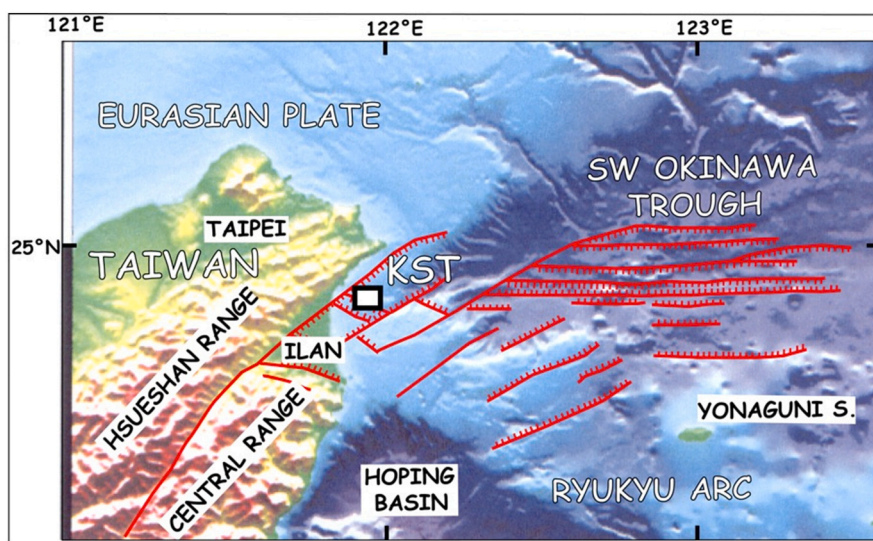


Fig. 1. Location of the Kuei-Shan Tao volcanic island (KST). Notice its situation in between the Ilan plain (onshore NE Taiwan) and at the SW tip of the Okinawa Trough; (Yonaguni S.: Yonaguni Sima/island). The major structures (red heavy barbed lines) come from Deffontaines et al., 2001). (For interpretation of the references to colour in this figure legend, the reader is referred to the web version of this article.)

erode. Andesite flows show an increase of thickness approaching the center of eruption.

- The Agglomerates or Pyroclastic Flow (PF for Chiu et al., 2010) are composed of small, thin and clast-supported angular blocks and lapilli of the previously described andesite lava flows facies (unaltered and weathered) with glass fragments cemented by tuffaceous

materials. Each Agglomerate (PF) layer seems coarsely sorted with larger andesite block at the base and become fine grained and even-sized to the top. With regards to the thicknesses of Kuei-Chia Agglomerates, one may notice that contrasting to the lava flows, they decrease upward and thicken downward (see for example the A-B geological cross-section on Fig. 2A). The PF should come from «

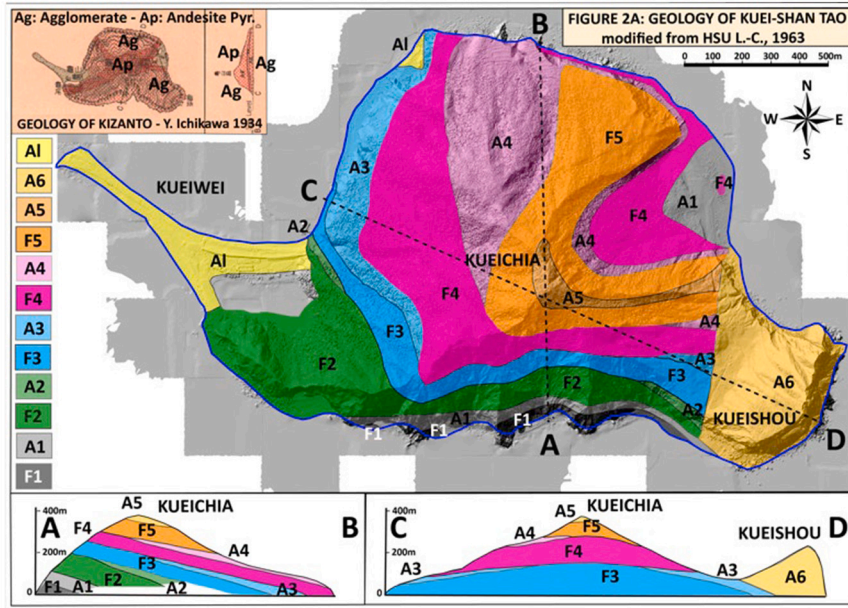
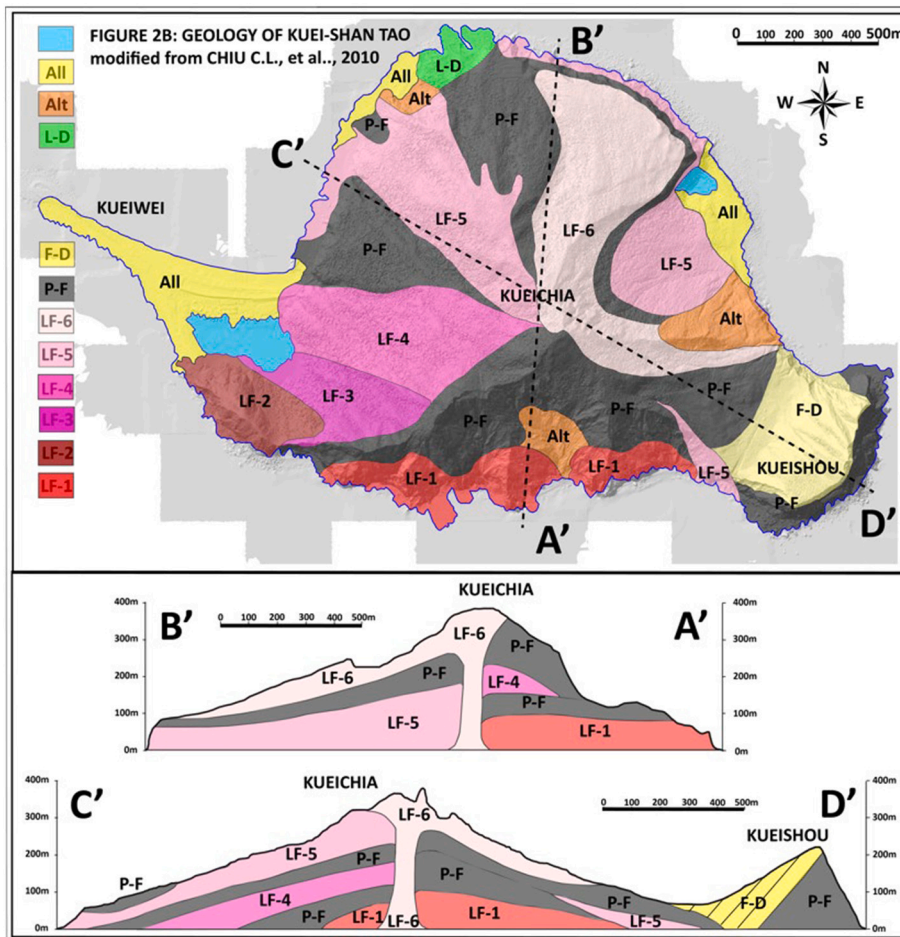


Fig. 2. Published geological mapping of Kuei-Shan Tao volcanic island. Both figures have the UAS-DTM hill-shade in background. A: KST Geological mapping modified from Hsu (1963): AI: Alluvium; An: Agglomerates; Fn: Flows with n ranging from n = 1 (older and outcropping base of the volcanic edifice), up to n = 5 (the last eruption lithological alternance). A-B and C-D representative geological cross-sections. Top left quadrangle: First « Kizanto » geological mapping of Yuichi Ichikawa, 1934 – detailed from « Toi » Geological map - N°15. B: KST geological mapping modified from Chiu et al. (2010): All: Alluvions; Alt: Alteration; FD: Fall deposits; PF: un-differentiated Pyroclastic Flows; LFn with n from 1 (older LF) to 6 (latest lava flow). Quadrangle in blue: lake. Same representative Geological cross-sections A'-B' & C'-D': One may compare Fig. 2A and B especially the inferred geometries of the volcanic deposits as the absence of faults. (For interpretation of the references to colour in this figure legend, the reader is referred to the web version of this article.)



small » explosion of the summit of the volcanic neck (Chiu et al., 2010).

- The xenoliths are ubiquitously and randomly distributed in both Flows and Agglomerates. They are composed of cordierite-pyroxene hornfels (gray or brownish colour, dense and compact, with quartz grain, patches of cordierite, diopside pyroxene, biotite, even sphene may be recognized with hornfels), wide distribution of quartzites, and some diopside-quartz-schists grain, corundum-spinel-gedrite-cordi rite rocks and some black streaks of graphite and sandy pelite. The study of xenoliths (caught during the ascension of the andesitic magma) is of major importance as they consist in the unique way to get to the KST basement lithology. The latter should be the same than the NE Taiwan as Quartzite and Quartz hornfels xenoliths show the same petrography than the sandstones and shales of the Paleogene strata and of the metamorphic rocks of the NE Taiwan.

Dealing with Kuei-Shou volcano (the « head of the turtle » situated at the eastern tip of the island), it is made of thick bedded « Agglomerates » with the same mineralogy than Kuei-Chia. The blocks of the lower part of the edifice are coarse and angular contrasting to those gradually finer at the top (200 m high). They are clearly overlying above the F3-A3 lithological alternance on the C–D geological cross-section (see Fig. 2A - Hsu, 1963) and should be overlying the more recent Kuei-Chia lava flow (F5) by interpreting its geological map. Consequently Kuei-Shou is the last KST volcanic activity.

On the structural point of view, Hsu (1963) notice only on the northern flank of Kuei-Chia few minor normal faults radially distributed less than 5 m vertical offsets. Hsu (1963) mentionned what he interpreted as the collapsed crater rectangular in shape which is a coarse preliminary description of the graben that we will describe hereafter. Chiu et al. (2010) also highlight the SW dipping of some Kuei-Chia lava flow which lead them to locate the Kuei-Chia eruptive center at the summit of the island. Consequently, the volcanic Kuei-Chia volcano appears to be highly dissymmetric in all directions with a volcanic feeder (LF6 - see the geological cross-sections) situated at the Kuei-Chia summit.

On the hydrothermalism point of view, the formation situated in the Kuei-Chia southern cliff is locally mineralized and recemented with irregular veinlets and joints of anhydrite, gypsum, and epidote due to hydrothermal percolations and alterations (Hsu and Ku, 1962). The three areas (NW, E and South of Kuei-Chia) of hydrothermally altered rocks are also enriched in chalcidony and christobalite silicate minerals, Chiu et al. (2010).

From the geomorphological and erosional point of view, Chiu et al. (2010) noticed some lahar deposits, which are composed of eroded volcanic rounded materials poorly sorted and transported by watersheds especially on the northwest and Western flank of Kuei-Chia. Moreover, a concave edifice was described in the NE flank (Chiu et al., 2010, see their Fig. 2) which they may interpret as the onshore crown of a landslide.

## 2.2. Previous geological mapping

Three geological mapping had already been published on Kuei-Shan Tao. The oldest one had been settled by the japonese Yuichi Ichikawa (1934) see Fig. 2A quadrangle top left: « Kizanto » geological mapping, 1:50,000 scale, « TOI » sheet - N°15; « Toi » is now Toucheng city situated in the Ilan Plain. Y. Ichikawa (1934) distinguished only two vertical lithological alternance of Tuff agglomerate (equivalent of the Agglomerate of Hsu (1963) or Pyroclastic Flow of Chiu et al., 2010) and Two pyroxens (augite and hypersthene) andesite (plagioclase feldspar andesine) with a glassy groundmass (Lava Flows). For Y. Ichikawa these formations are coarsely flat lying as shown on the C–D geological cross-section with lateral variation of Tuff agglomerate thicknesses.

Since then, Kuei-Shan Tao has conducted two detailed geological mapping (Hsu, 1963; and Chiu et al., 2010). Their description help to decipher the geological arguments and facts put forward by these

authors. The Geological mapping of Hsu (1963) appear to be influenced by the N-S topographic dissymmetry of the Kuei-Chia edifice. Kuei-Chia has a slightly sloping northern flank underlain by volcanic strata contrasting with the very steep southern flank. The southern flank of the volcano is missing (see also Fig. 2 A-B geological cross section). Hsu (1963) distinguished five alternance of associated Flows and Agglomerates on the northern flank of Kuei-Chia volcano. He noticed their same mineralogical and chemical compositions suggesting a volcanic setting within a short-inferred Pleistocene time period. Hsu also note that the strata are dipping parallel to the topography with dip angle varying from 15 to 20° radially north, east, and west of Kuei-Chia which implies that the volcanic neck (the feeder or the volcanic center) is situated close to the south of the island. Chiu et al. (2010) conducted the last 1:5000 scale geological map, using the 2 m ground resolution LIDAR Digital Terrain Model of the Central Geological Survey in order to reconstruct the KST volcanic sequence. On Kuei-Chia, they newly distinguished six Aa Lava Flows (LF below) with brown reddish surface from LF1 (base of the edifice) up to the latest LF6 (that corresponds to the F5 of Hsu, 1963). They interpret LF2 (SW of Kuei-Chia) as a lava dome with volcanic organs with cooling joints.

Looking more carefully those geological mappings shows inconsistencies. For instance, one may notice on Chiu et al., 2010 that LF2, LF3 and LF4 are situated only on the southwestern side of the Kuei-Chia edifice close to the Kuei-Wei lake. It seems also difficult to distinguish the relative ages of those three massive lava flows. Another example show close to the southern shoreline West of Kuei-Chia, LF3 is mapped below LF2 (so LF3 should be older than LF2!). One may also note the lack of lithological continuity on both sides of the crest south of the Kuei-Chia summit. Moreover, on this geological mapping the pyroclastic falls are not differentiated and not associated with Lava flows. One may note also the great variation of thicknesses of LF5 on the two geological cross-sections (Fig. 2B A'-B' & C'-D').

Dealing with Kuei-Shou, Chiu et al., 2010 confirm Hsu (1963), the independant volcanic Kuei-Shou edifice is overlying above Kuei-Chia LF5 (see the eastern part of the geological C'-D' cross-section on Fig. 2B) so Kuei-Shou erupted later than LF5. The bedding of the western part of the Kuei-Shou edifice is generally dipping 25° to the West. We know now, from bathymetric sea surveys and dives that the missing part had just been eroded forming a flat eroded marine terrasse just below the sea level which is the result of the high erosional actions of the Kuroshio sea current against soft non-consolidated Kuei-Shou Agglomerates. Kuei-Shou edifice is composed of Pyroclastic Flow at the base and Fall-Deposits at the top. Contrasting to the drawings of Hsu (1963) where the Kuei-Shou deposits parallell the topography, on the Chiu et al. (2010) C'-D' geological section the volcanic deposit appear to be oblique to the topography (looks like truncated?) and so seems to have been eroded which is not the case in the fields (see below Fig. 2 & Hsu, 1963).

## 2.3. Inputs from the Kuei-Chia cores (drilling GSI-01A & 01B)

The northern flank of the Kuei-Chia volcanic edifice had been drilled by the Taiwan Central Geological Survey (MOEA) with two complementary closed by cores GSI-01A and 01B (see Fig. 3) were summarized and located by Chiu et al. (2010). Core A give a description of the volcanic strata from the surface to -140 m depth whereas core B completed the previous core from -70 m and extend down to -290 m. Chiu et al. (2010) distinguished twelve (12) layers of lava flows interlayered with Pyroclastic Flows and lahar deposits. In addition, numerous xenoliths had been evidenced and are increasing from -110 m up to the surface.

We have re-interpreted herein the core GSI-01B from the initial field observations, whereas Core GSI-01A is only slightly modified from Chiu et al. (2010) observations. From these two cores we deduce the following succession of a typical volcanic sequence of a Kuei-Chia eruption described below from bottom to top: at the base it is composed of a volcanic breccia then above a massive lava flow (MLF or LF) with sometimes at its top a layer of columnar lava flow that is made

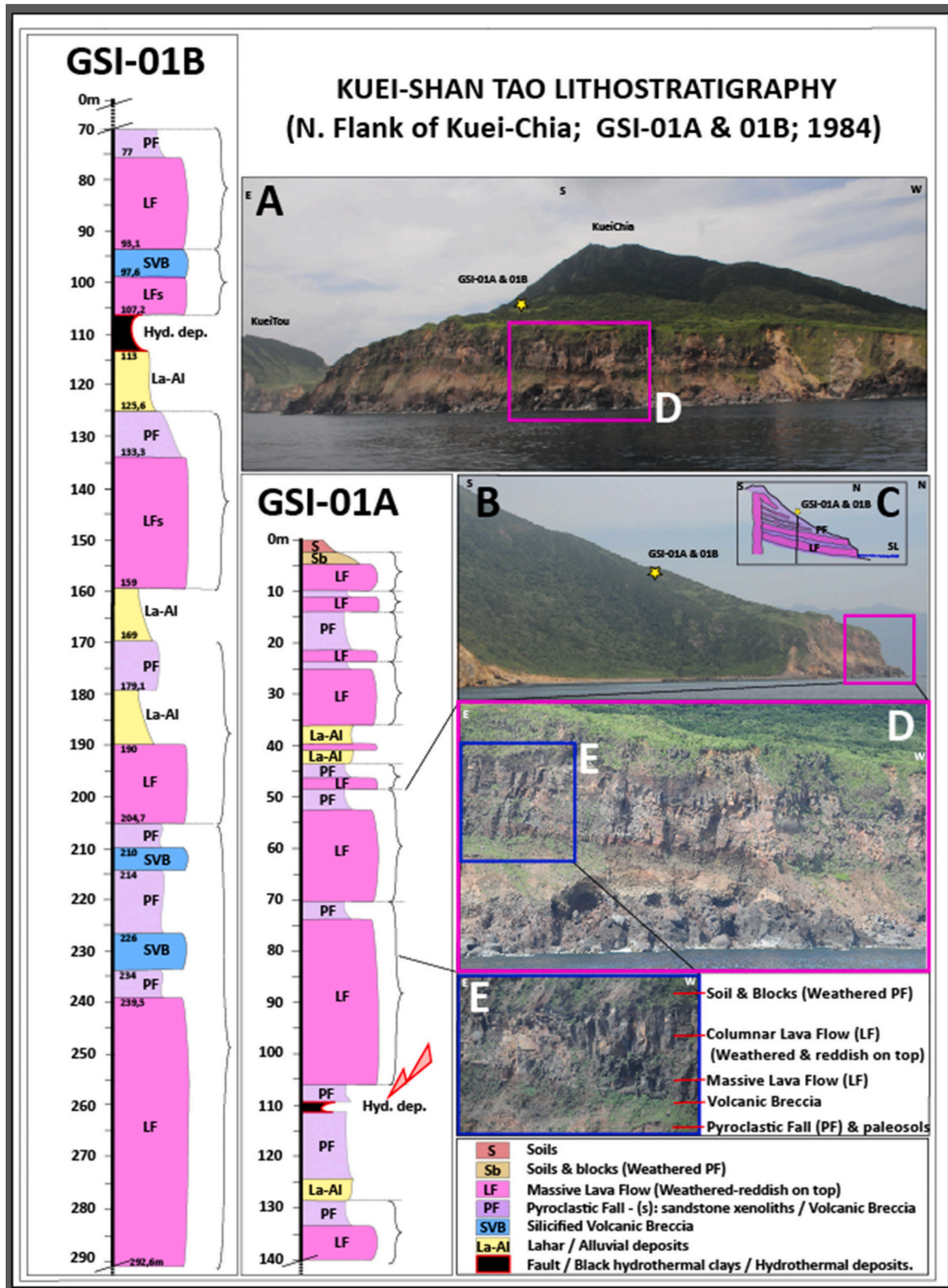


Fig. 3. Core GSI-01A (description from Chiu et al., 2010) and Core GSI-01B from the northern Flank of Kuei-Chia. Fig. 3A and 3B photographs that locate the drilling area (yellow star) and the down-stream outcrops at the sea-cliff. Fig. 3C: Inferred structural scheme of the massive lava flow and pyroclastic flows that may link the outcrops and the two cores. Fig. 3D: General view of the Sea cliff showing the lithological alternance of massive lavaflow and Pyroclastic falls; Fig. 3E: Detailed KST typical volcanic sequence. From base to top: volcanic breccia (beginning of the eruption with degassing, base of the lavaflow reworking pre-existing materials), massive lava flow, columnar massive lava flow (columnar when it is quickly cooling), then Pyroclastic flow/fall (PF, corresponding to volcanic ash deposits associated to the decreasing of the volcanic eruption activity) with then development of soil on top of PF and vegetation growing (quiescent period in between two volcanic crisis). (For interpretation of the references to colour in this figure legend, the reader is referred to the web version of this article.)

by numerous cooling joints. Above it, there is Pyroclastic Fall (PF) (and not Pyroclastic flow) deposits that consist of a large coverage of volcanic ash deposits. Soils/Paleosoils develop on top of the PF corresponding to quiescent volcanic periods (see Fig. 3A, B, C, D & E).

One may notice the presence at depth around -110 m on the two cores of the presence of a black hydrothermal clay level characteristic of a major fault plane (inferred as corresponding at depth to an eastern dipping NE-SW trending normal fault). The three silicified volcanic breccias (in blue, Fig. 3) on core GSI-01B are interpreted as faults associated with percolation of fluids from deep origin. Based on the thicknesses, we propose to link the thickest volcanic series to the one outcropping at the sea-cliff of the northern KST shoreline. The major point is that we get herein a vertical lithological succession of the Kuei-Chia northern flank through these two cores.

The previous KST geological mappings lack the structural point of view as no dips, nor faults had been recognized and located. As KST structural field work is difficult due to both military restrictions and high cliffs so it is impossible to access by boat, we decided to use UAS to get a precise topography of the edifice. We consequently proposed herein to up-date previous works using the structural analysis of our new hillshade high resolution UAS DSM in order to provide a detailed structural sketch map associated with the KST neotectonic map. Below then we precise the way we get the UAS DTM and how we made the morphostructural analysis in order to propose a KST structural sketch map.

### 3. First Kuei-Shan Tao UAS survey

An airborne Lidar Digital Terrain Model (2 m ground resolution) had been acquired all around Taiwan generated for the Central Geological Survey of the Ministry of Economic Affairs (CGS-MOEA). But this Lidar DTM has strong access restrictions and it is not available for foreign scientists. Consequently, we decided to acquire, process and analyse a new high-resolution digital terrain database from our UAS/drones.

In order to get the UAS High Resolution Digital Surface Model (UAS-HR-DSM hereafter) of the volcanic Kuei-Shan Tao, we carried out a photogrammetric survey in June 2017 from the Ilan coast plain, about 10 km distance from KST. Our final HR UAS DSM is much more precise (7.5 cm ground resolution (GR) to compare with the 2 m GR of the Lidar DTM) which is so convenient for a structural analysis.

From a technical point of view the drone used in this study was a modified already-available Skywalker X8 fixed-wing aircraft reinforced by carbon fiber rods and Kevlar fiber sheets. Launched by hand, flies, takes photos, and landing autonomously by using a pre-programmed flight plan. The autopilot system is composed and modified from the open-source APM (ArduPilot Mega 2.6 autopilot) firmware and open-source software Mission Planner, transmitted by ground-air XBee radio telemetry. The Sony ILCE-QX1 camera and 16 mm SEL16F2.8 lens was used, > 85% endlap and > 55% sidelap by autonomous equal distance in fly mission. The flight missions were planned with 200-400 m above ground level (AGL). Overall 597 photos were matched, adjusted and for model reconstruction from a total of 619 images. The data sets, including orthomosaic images (Fig. 4A), Digital Surface Model (Fig. 4B & 4C, DSM hereafter), and true 3D model, were generated and processed by ContextCapture commercial software with a grid spacing of 7.5 cm. By using rigid registration of photo positioning data, global errors after aerotriangulation from automatic tie point for 169,637 total number of points, average of 1399 points per photo, and a median number of 4 photos per point. The root mean square (RMS) of reprojection errors is 0.55 pixel. The RMS of distances to rays is 0.068 m. In this study, we have used the same drone than in Deffontaines et al. (2017, 2018 and 2019), Chang et al. (2018) and Mouyen et al. (2020). To get more processing information refer to Chang et al., 2018; Deffontaines et al. (2016, 2017, 2018, & 2019).

The final UAS-HR-DSM ground planimetric resolution corresponds to a ground sampling distance (GSD) of 7.5 cm and the total area covered is about 2.7 km<sup>2</sup>. Unfortunately, we were not able to validate our UAS-HR-

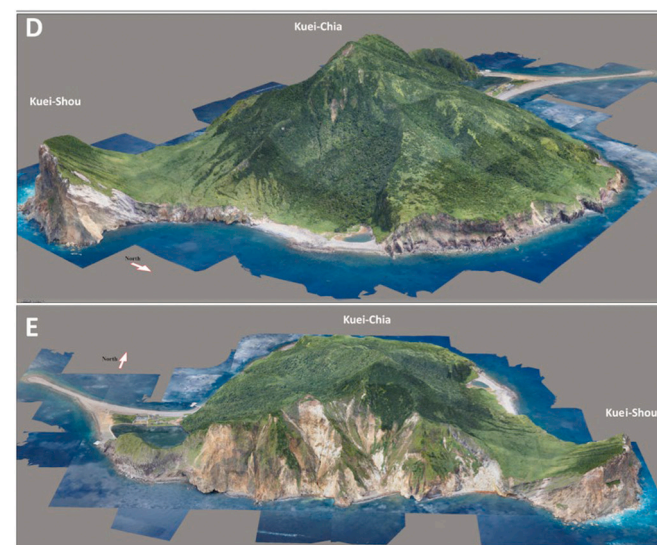
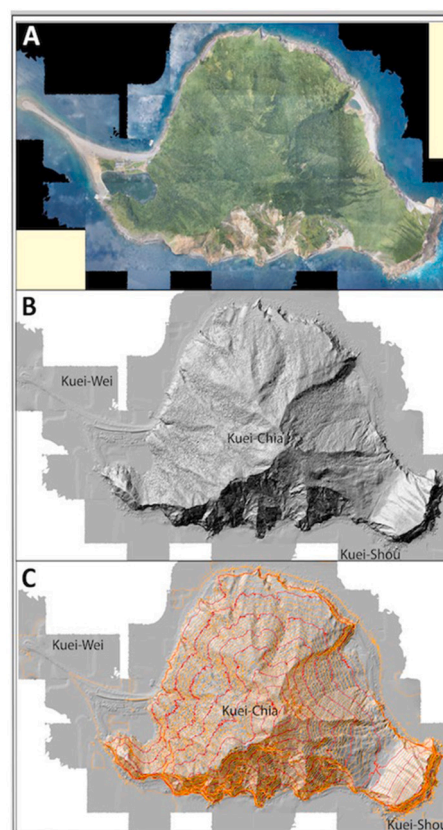


**Fig. 4.** UAS high resolution orthophotos and digital surface model of Kuei-Shan Tao: Fig. 4A: KST Orthophotos mosaic. One may note the grayish/yellowish areas that correspond to erosion areas in the southern shoreline contrasting to the general vegetation coverage in green. Fig. 4B: Black and white UAS HR DSM hillshade (light from the NW, no vertical exaggeration); Fig. 4C: Isocontours (vertical equidistance: 10 m for the isoaltitude orange lines whereas the isoaltitude red lines are each 50 m) superimposed to the black and white UAS HR DSM hill shaded (with a transparency). Perspective views of the KST UAS HR DSM covered by the orthophotos view from the NE (Fig. 4D), and view from the south (Fig. 4E). (For interpretation of the references to colour in this figure legend, the reader is referred to the web version of this article.)

DSM by Ground Control Points (GCP's) nor previous topographic survey on the island due to restricted area for military reasons. That is why we have only processed herein the Digital Surface Model (DSM), and highlighting both the ground and the top of the vegetation (when it is covered) and not only the Digital Terrain Model (corresponding to the ground surface). But our long-time experience and our numerous previous UAS surveys reveal a planimetric accuracy of 7 to 12 cm and a vertical accuracy less than 40 cm.

The Fig. 4A (KST mosaic orthophotos), 4B (KST black and white hillshade DSM), 4C (KST topographic isocontours above the B&W hillshade), highlight planimetric views; whereas Fig. 4D and E illustrate two 3D-views from both north and south of our new KST UAS DSM.

This high resolution UAS survey allow us to do a structural sketch map using a detailed photo-interpretation and morphostructural analyses (Deffontaines, 1991; Deffontaines and Chorowicz, 1991; Deffontaines et al., 1992a,b, 1993, 1994...) to define structures that affect the topography, which are validated locally by the observations of coastline topographic outcrops from a boat.

With a decimeter ground resolution Digital Surface Model, it is possible to analyse and propose an updated geological mapping of the KST volcanic cone using the geometry of the topographic isocontours, the decametric vertical displacement of the volcanic strata of the outcrops all along the KST shoreline as well as the thicknesses of the different lava flows. We will first refine the morphostructural analysis methodology used herein before applying it to the KST.

#### 4. Morphostructural inputs

##### 4.1. Morphostructural principles

Based on the previous geological observations and mappings, and in order to interpret the high resolution (HR) UAS DSM, we have applied herein the morphostructural principles of geological mapping in a volcanic edifice environment:

1. Lava flows and pyroclastic falls are deposited radially all around the volcanic cone from the caldera summit providing parallel topographic concentric isocontour centered on the volcanic caldera.
2. Lava flows run perpendicular to the topographic isocontour lines, from the caldera following the initial down-dip slope directions toward the sea following the shortest way.
3. It is possible to locate the caldera by tracing perpendiculars to the parallel topographic isocontour or contour lines of the volcanic flank.
4. The structural surface of pyroclastic falls deposits smoothed the topography contrasting to the slightly hummocky and chaotic top of Aa massive lava flows.
5. Active weathering and pedological processes smoothed quite rapidly the volcanic flanks of volcanic edifice situated in tropical climate.
6. Dealing volcanic Pyroclastic falls deposits thicknesses: we infer that thickness of pyroclastic fall increase downwind of the dominant winds directions. Pyroclastic falls are sorted and their thickness decrease slightly from the caldera (top of the edifice characterized by proximal, larger blocks) to the bottom (distal finer deposits).
7. Lava flows thickness might vary downward of the volcano due to the decreasing of slope, flow reduction, the cooling of temperature, the lateral lava spreading storage downward, etc.; Due to the fluidity of the lava flow, we infer also that thick lava flows have a larger lateral extension downward.
8. Watersheds/Rivers/Talwegs are flowing radially from the top to the bottom of the volcano following the shortest way and the deepest slope perpendicular to the topographic isocontours. They

should present the same incision on both sides. Those rivers may be used by lahars deposits sedimented all along and downstream.

9. Unique/isolated steep slope separating two dipping sub-rectilinear planimetric surface may correspond to the lateral edge of lava flows, or recent tectonic fractures and faults that split and offset the same lava flow. Then we interpret offset of parallel isocontours which are not centered to the caldera, by vertical faults that offset the same volcanic lava flow.
10. Watershed/rivers flowing obliquely to the parallel topographic isocontours are obviously guided by alternance of lithologies, faults or landslides (see below and Deffontaines et al., 1992a, 1992b, 1993, 1994, 2016, 2017);
11. A landslide should be characterized by numerous parallel topographic isocontours which are oblique to the regional radial down-dip slope AND does not fit with the inferred location of the caldera, AND are bounded by rivers with an « horse-shoe concave shape to the sea geometry corresponding to the crown of the landslide.

Applying these morphostructural principles to the KST volcanic island, we were able to simplify the geometry of the volcanic apron by adding fractures and faults that offset the volcanic deposits.

The detailed morphostructural analysis of the topographic isocontours (Fig. 4C) with a 10 m vertical equidistance helps to get to the general structural overview of the KST volcano. For instance, the planar areas (planeze) with parallel isocontours radially distributed toward the summit (the caldera) should correspond to structural surface of lava flow and Pyroclastic Fall (quadrangle 1, 2 and 3 of Fig. 5). The quadrangle 4, 5, 6 and 7 highlights normal faults that affect the topography with 2 beheaded rivers situated on the northeastern flank of Kuei-Chia. The fracturation observed from the quadrangles 8 to 13 corresponds to normal faults revealed by the detailed analysis of the HR UAS-DSM on the southern and eastern flank of Kuei-Chia (see especially the 3D sketch-views 9 and 11). Those normal faults may be also re-activated by landslides if they are facing a suitable erosive potential, they should be re-activated as crown of landslides (quadrangle 8 and 10). Landslides have typical upstream « horse-shoe » shape geometry corresponding to the landslide crown. The latter is characterized by a U-shape connected steep slope with a concavity directed to the dip-slope. It is often highlighted by the arcuate planimetric geometry of the drainage pattern (see the NE and NW part of Kuei-Chia and quadrangle 13). The upper part corresponds to the outcropping sliding surface (normal fault due to gravity). Moreover quadrangle 13 to 17 highlights the presence of vertical massive lava sheet which is interpreted as a vertical fresh volcanic dyke within the weathered/alterted southern flank of the Kuei-Chia volcano. The quadrangle 18 (Fig. 5) shows a set of two normal faults that affect both NNE and W flanks of the Kuei-Chia volcano.

Certainly, this morphostructural analysis present uncertainties: for instance, the UAS-DSM without ground control point (GCP's) provides the canopy of the vegetation and consequently does not provide with great accuracy and precision the lava flows boundaries, edges, lateral and maximal extension. Consequently, it is difficult to distinguish the different volcanic sequence from this UAS-DSM only despite its decimetric high resolution. But in another way the vegetation is in an « equilibrium state ». Most of Kuei-Chia is covered by the same species with same hight, same maturity, without human actions in this military area with strictly restricted access. So the DSM should reflect the ground surface (digital terrain model - DTM). Most of the structures cited herein had been also confirmed with structural arguments taken from a near shoreline morphostructural survey of the sea cliffs and all the KST flanks from the famous « Ocean Researcher 1 » first oceanic Taiwan research vessel. There is no possibility to get to the elongated and narrow boulders beaches situated at the base of the sea cliffs.

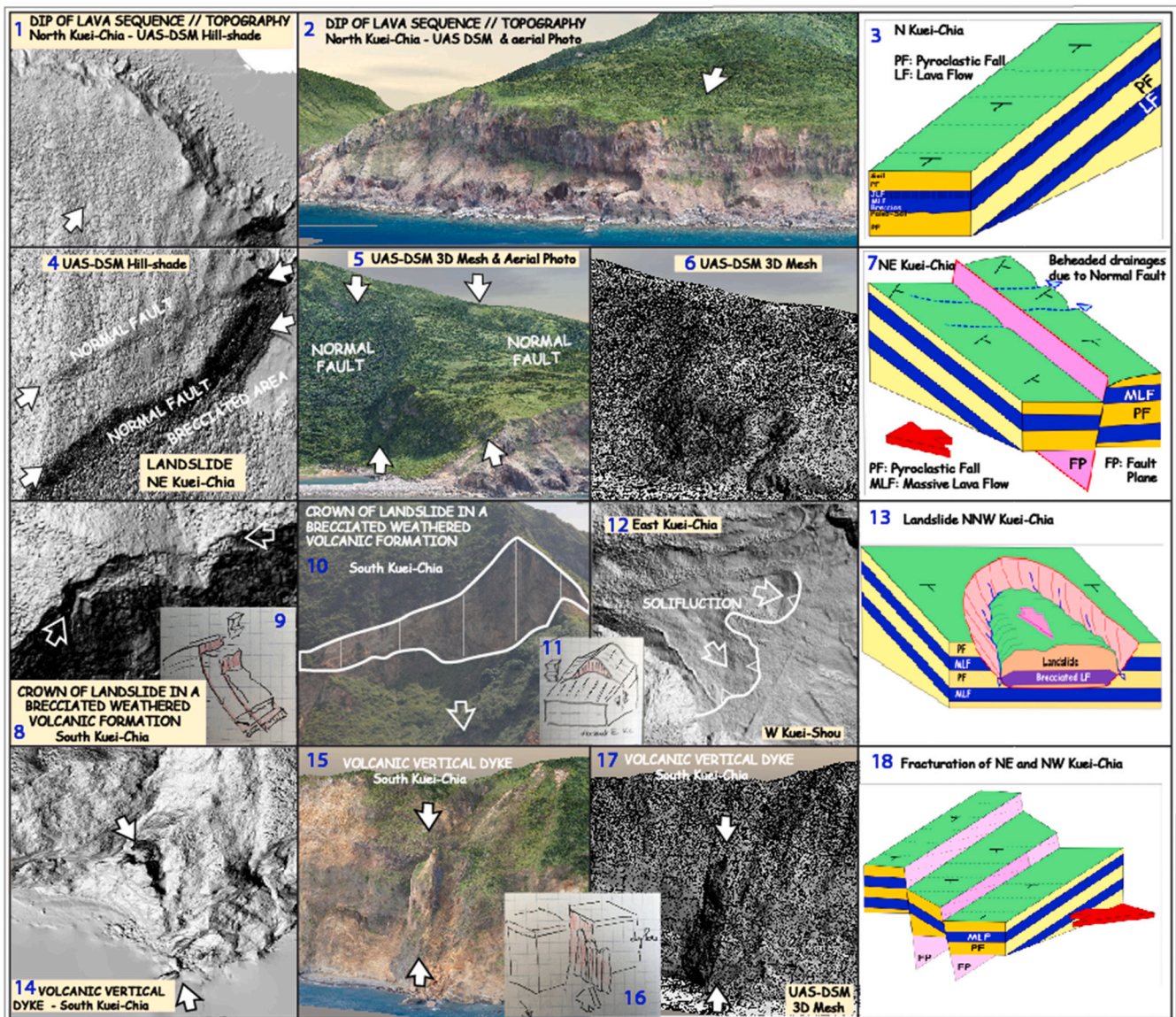


Fig. 5. Example of morphostructures on Kuei-Shan Tao volcanic cone.

Quadrangle 1, 2 & 3: A volcanic serie composed from bottom to top of a breccia, massive lava flow, columnar lava flow (LF), pyroclastic fall (PF) and (paleo)soil in northern Kuei-Chia; Quadrangle 4, 5, 6 and 7: Normal faults oblique to the cone with two beheaded rivers. Quadrangle 8, 9, 10, 11, 12, and 13 normal faults and landslides. Quadrangle 14, 15, 16, and 17 vertical dyke. Quadrangle 18: Fracturation multiple on NE and W Kuei-Chia.

#### 4.2. Summit level map applied to Kuei-Chia volcano

So, we first draw a theoretical volcanic cone using concentric green isocontour lines that best fit the geometry of all the topographic isocontours of the volcano. We infer that the topographic isocontours also correspond to structural surface (top fo the PF – see Fig. 2, 3 and Fig. 6). It is like to create a « summit level map » of the volcanic cone (see Deffontaines, 2000). The location of Kuei-Chia caldera is then revealed and is located with a heavy black circle close to the Kuei-Chia summit (Fig. 6). Then we qualitatively analyse the direction of the topographic isocontours toward the summit level green lines that characterize the theoretical KST volcanic edifice. We infer that as soon as their directions diverge for more than  $45^\circ$  it means that there are obviously guided by an external factor such as the tectonic or a slide (Deffontaines et al., 1992a, 1992b, 1993, 1994, 2001). We especially focus herein on both drainage network and dips of the DSM surface. Then on Fig. 6 the dips in black are coherent with the caldera situated on top of Kuei-Chia contrasting to the dips in red which are inconsistent with the inferred location of the

caldera. Moreover, we draw the drainage in blue that fit with the theoretic radial centrifugal drainage of a volcanic cone. But we highlight in black the anomalous drainage which does not fit with the theoretic volcanic cone (green isocontours) flow direction. Anomalous red dips and black drainage are guided by tectonic structures, or erosional ones. In order to distinguish in between both interpretation we followed the morphostructural principles described in the paragraph 4 above and we propose the following structural scheme above the Kuei-Chia summit level map (Fig. 6). The anomalous drainage of the SW part of Kuei-Chia correspond to the dismantling of the southern part of the Kuei-Chia volcanic edifice as previously suggested by Hsu (1963, « collapsed crater »). Consequently, using the morphostructural principles cited above we are able to locate, characterize, and partially quantify faults (heavy red lines of Fig. 6 with ticks on the downthrown side) and landslides (light transparent red areas in Fig. 6).

Moreover, from Fig. 6, we distinguished in Kuei-Chia two different kind of landslides: (1) a massive lava flow sliding above the pyroclastic flow and ash falls acting as a sliding surface in northern Kuei-Chia (see

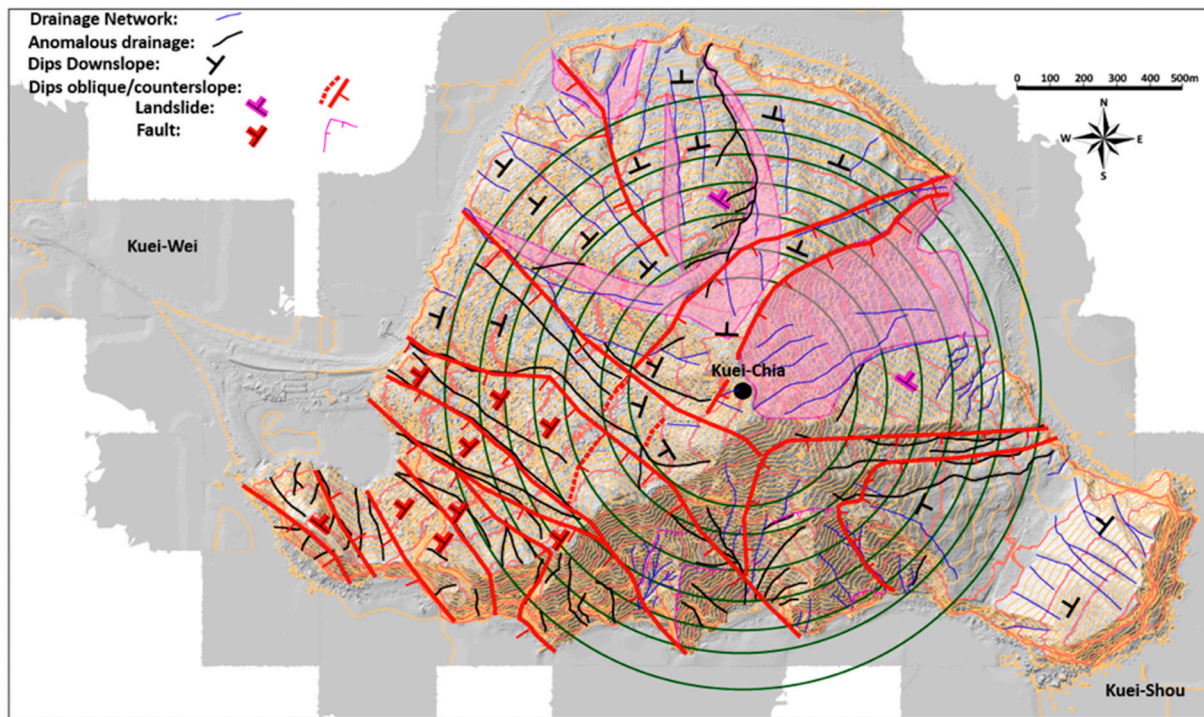


**Fig. 6.** Summit level map of the Kuei-Chia volcanic cone (green lines that best fit with the topographic isocontours situated all around the volcano). Heavy black point: Inferred Kuei-Chia Caldera / summit; Blue lines: normal drainage network flowing perpendicular to the green summit level lines. Black lines: anomalous drainage that flow obliquely to the theoretical volcanic cone (green lines). Dips in black: lava serie flowing normally from the caldera following the shortest downstream dip slope to the shoreline. Dips in red: Anomalous dips individualizing faulted blocks. Dips in purple: anomalous dips highlighting inferred rotational or plan landslides. The southern flank of Kuei-Chia is weathered and altered (Hsu, 1963). (For interpretation of the references to colour in this figure legend, the reader is referred to the web version of this article.)

also Fig. 5 quadrangle 13 for the 3D view); and (2) a more important landslide in the NE part of Kuei-Chia (Chiu et al., 2010, and Huang et al., 2021). Whereas close and linked to the Kuei-Shou volcanic activity, we noticed only solifluction processes affecting the Pyroclastic falls (see Fig. 5 quadrangle 12).

The summit level map leads us also to estimate the total volcanic volume emitted by Kuei-Shan Tao which is  $0.434 \text{ Km}^3$  above sea level. Two terrasic levels had been recognized all around KST below sea level (see figure Huang et al., 2021) that might correspond to the base of the volcanic edifice at  $-60 \text{ m}$  which provide a volcanic volume of  $0.797 \text{ km}^3$ , and the deeper terrassic level at  $-140 \text{ m}$  providing a volcanic volume of  $2.08 \text{ km}^3$ . One may bear in mind that the Kuroshio Sea currents erosion is not taken into consideration herein consequently they correspond to minimize the volcanic volumes.

The summit level surface (Deffontaines, 1985 and 1991) applied to recent volcanic cones reveal the location, the characterization and quantify the active faults that affect the volcanic edifice. This method should be applied to other volcanic edifices in order to prove its structural and landslide interest.

## 5. Kuei-Shan Tao structures from a boat

In June 2017, an oceanic survey onboard R/V Ocean Researcher Number 1 (Taiwan) was supervised by both S-K.Hsu and P.Huang (Oceanographic Lab. National Central University) all around Kuei-Shan Tao. Numerous Sparker seismic profiles were acquired that lead us to get a whole geological bird's eye view of the offshore structures (Huang et al., 2021). During that offshore survey, the northeastern and the southern shorelines were then precisely monitored, observed and described only from the boat offshore as the outcrops situated at the lower part of the Sea-cliffs are practically impossible and highly dangerous to reach (see Fig. 7 and 8).

Contrasting to the previous observation lacking faults on the pre-existing geological mapping, we note the presence of numerous faults (red heavy lines) that offset vertically the continuity of the lithologies all along the sea-cliffs of the Kuei-Chia northern flank (bird's eye view Fig. 7A and detailed of Kuei-Shou 7B, where white dashed lines correspond to lithological boundaries). Fig. 7C confirms that Kuei-Shou corresponds to the last KST volcanic episode as it is overlying Kuei-Chia deposits (already seen by Hsu, 1963, and Chiu et al., 2010). The heavy red surface corresponds to a major normal fault east dipping with numerous splays such as the 7D scarp. One may notice at sea that this area corresponds to numerous offshore volcanic events and fumaroles. Fig. 7E, 7F and 7G reveal the presence of numerous faults with decametric offset and their associated drag folds (see white dashed lines) on both sides of the fault plane (red lines) provides a clear normal fault motion. It is not possible to get the lateral displacement (if any) from these observations.

From the various outcrops situated along the northern KST shoreline (Fig. 7), we can photo-interpret and deduce the relative constant thickness of the massive lava flows that should reflect their relative fluidity and may explain their wide lateral extension around the volcanic Kuei-Chia edifice. Locally close to the fault zones, drag-folds modify the bedding revealing the normal motion on the fault planes and highlight the recent tectonic (as the last Kuei-Chia volcanic sequence is affected, Fig. 7E, 7F, 7G) and the landsliding activities (7A). Moreover, contrasting to Chiu et al. (2010), we have not recognized in the fields specific massive lava flow ridges. Some elongated ridges that we recognized are situated within a landslide and we interpreted those alignments as chaotic brecciated volcanic materials in the Kuei-Chia northern flank (see the ridges Fig. 5.1, 5.4, and on Fig. 6). Other ridges correspond to the lateral boundary of a rather flat landslide in northern Kuei-Chia (see Fig. 5.13).

The southern flank of KST is made of huge sea cliffs made of

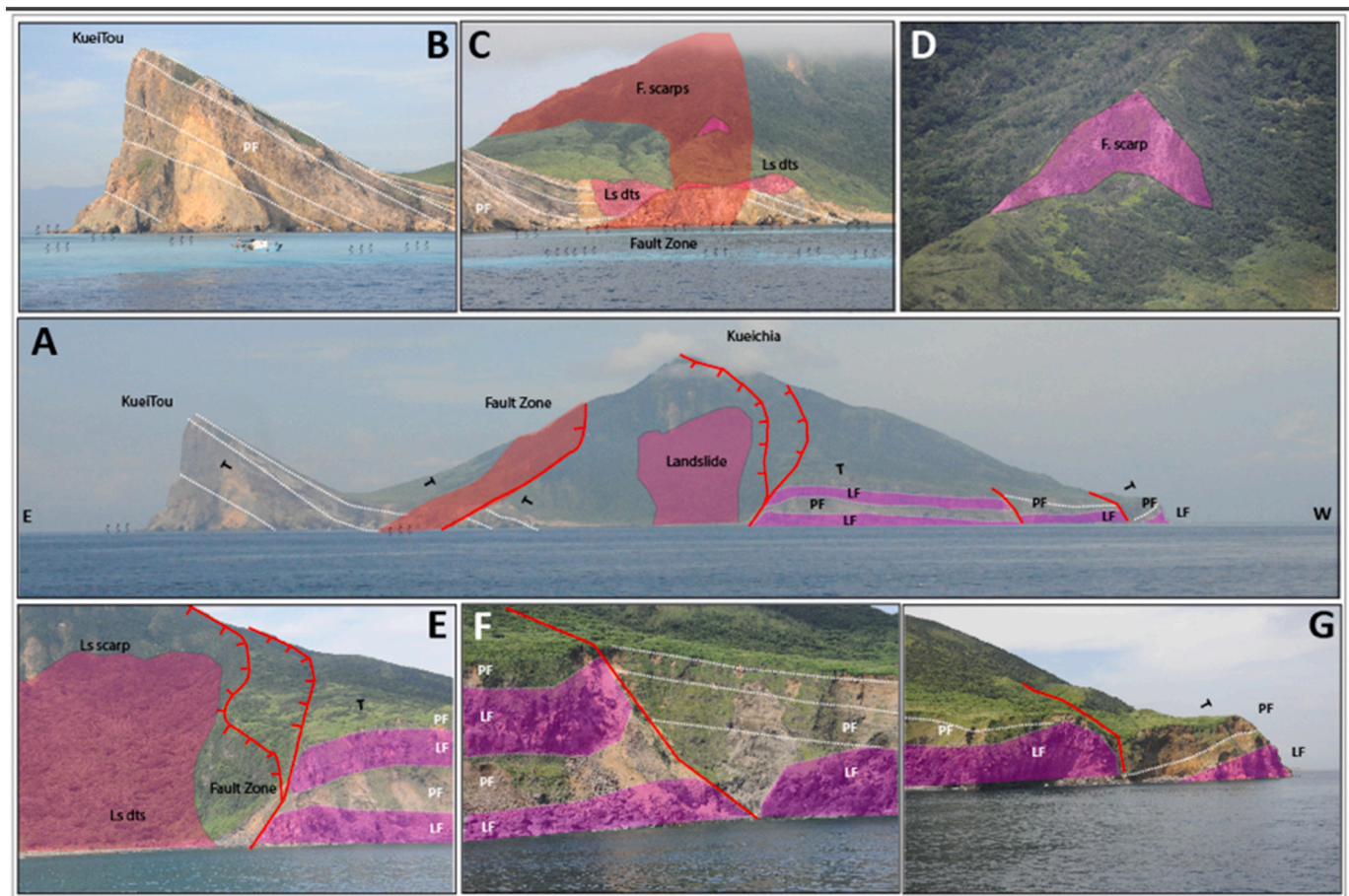


**Fig. 7.** Photo-interpretation of the northeastern shoreline of Kuei-Shan Tao: One may see the faults (heavy red lines/surface) that offset vertically the volcanic deposits; Normal fault with ticks on the down-faulted part and their associated drag folds, reddish zone: fault scarp, LF (purple areas, white letters): massive Lava flows; PF (white letters): Pyroclastic fall, the coarse sorting is highlighted by white dashed lines; Black T: bedding dips; Ls: Landslide scarp, Ls dts: landslide brecciated deposits.

previously described weathered volcanic materials (Hsu, 1963; Chiu et al., 2010). Our observations reveal the presence of numerous lithostratigraphic boundaries (white dashed lines on the detailed photographs) highlight by variations of deposits, different colours which are offset vertically by rather vertically dipping joints and faults (red lines and red surfaces) and some NW-SE trending volcanic dykes (purple surface) (see quadrangles 1, 2, 3, 5, 6, 7, 8, 9, 10 & 11). The trending of faults and dykes are deduced from the trending of the fault and dyke's planes surface. Some of them are trending NW-SE. Then these field observations from a boat support our previous UAS DSM analyses of a NW-SE vertical dyke (Fig. 5-14, 5-15, 5-16, 5-17). One may also notice the specific teeth morphology of the summit of volcanic dykes (top left quadrangle of Fig. 8, dyke situated south of Kuei-Chia that may be seen from the Ilan Plain). Moreover, it is normal from a geological point of view to find a continuity of the volcanic deposits on both sides of the crest of Kuei-Chia. The inferred sommital Kuei-Chia caldera (Fig. 6) corresponds to a becciated dyke (volcanic neck of the quadrangle 10). The southern flank is also affected by numerous landslides which increase the dangerousness of the access (Fig. 8-3 and 8-11).

To conclude, this photo-interpretation of the southern flank of KST from a boat clearly revealed the presence of numerous structures such as almost vertically dipping faults and volcanic dykes that offset vertically the continuity of the volcanic deposits all around KST island. Consequently, our aim herein is to precise the structural scheme and deal with their neotectonic activity. Then we combine our different previous observations in the following synthetic KST structural sketch map and propose below a model of its recent activity with the KST neotectonic

map.

## 6. Updated Kuei-Shan Tao geological mapping and neotectonic map

Taking into consideration the previous geological observations, and previous works, our new morphostructural analysis of the high-resolution UAS-DSM and structural field observations, we are consequently able to propose a structural scheme of the KST.

### 6.1. Lithological geometry

One may bear in mind that it is not possible to distinguish geometrically the different andesitic volcanic series drilled on the northern flank of Kuei-Chia from the used UAS-DSM dataset (see above). The latest Kuei-Shou pyroclastic falls have slightly covered the whole KST island that smoothed the topography and masked the superposition of the alternance of lava flows and pyroclastic falls. Moreover, it is difficult for us to connect the two cores A and B with the downstream outcrops on the shoreline (see the inferred correlation of core A and Fig. 3-D based on the same thicknesses of the two volcanic sequences).

So we decided herein to simplify all the conic volcanic series by using a single colour: O-VC for « old volcanic cone facies ». It corresponds to the outcropping volcanic series partially recognized within the 2 cores of Fig. 3. They have dips (T in black, Fig. 8) dipping normally along the downward slope of the Kuei-Chia volcano. The southern part of the volcanic cone is missing. It is down faulted by numerous NW-SE vertical

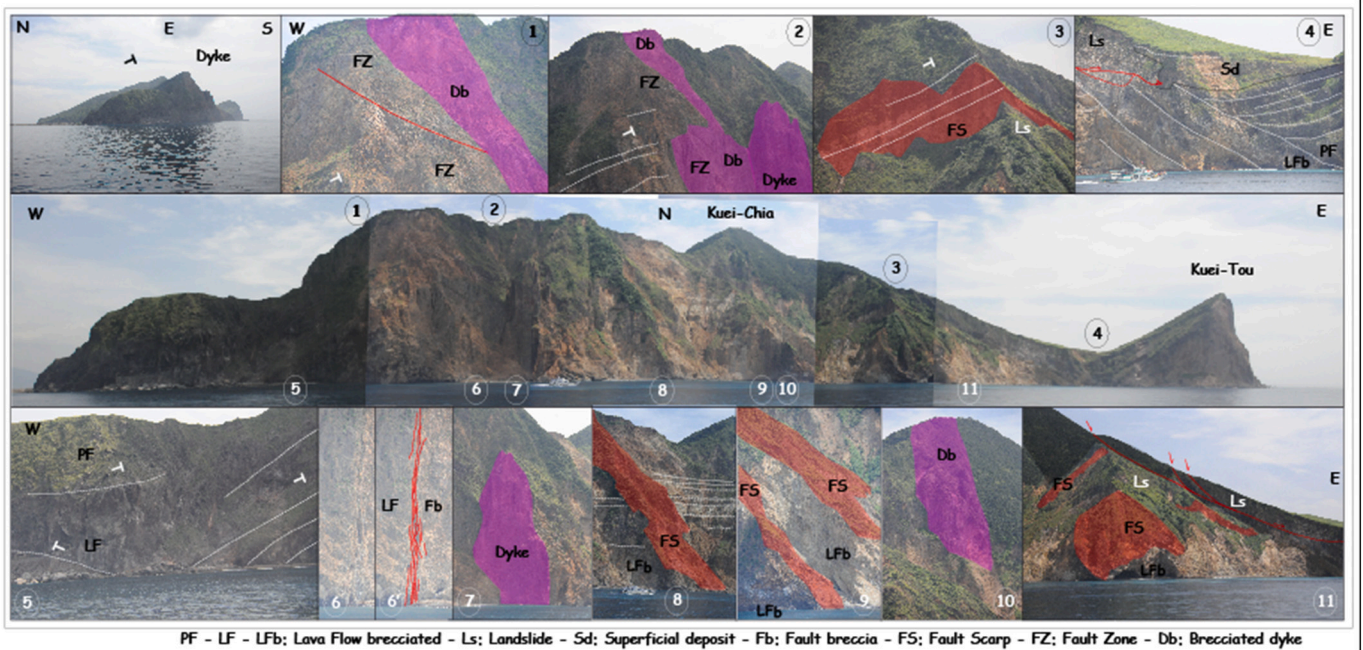


**Fig. 8.** Photo-interpretation of the southern shoreline of Kuei-Shan Tao (photographs taken from the boat): as for [fig. 7](#) the central photograph gives the bird's eye view of the southern KST flank and shoreline. The photographs situated on top and bottom lines have a number located on the central full view. They precised specific structural views that document the morphostructural analysis above. The top left picture shows the dissymetry of the Kuei-Chia volcano with a structural surface slowly dipping to the north contrasting to the scarps and sea cliffs of its southern shoreline. The white dash lines highlight the stratigraphic volcanic sequence. The red lines or surface correspond to fault zones. The purple surface corresponds to the inferred vertical dykes that offset the stratigraphic boundaries. Faults/Fault Zone (FZ) (heavy red lines); Fb: Fault brecciated; Fs (red areas): Fault Scarp; Db: brecciated dyke; Ls: Landslide scarp, LF purple areas: massive Lava flows LFb Lava Flow brecciated; PF: Pyroclastic fall, Sd: Solifluction deposit; Black and white T: bedding dips.

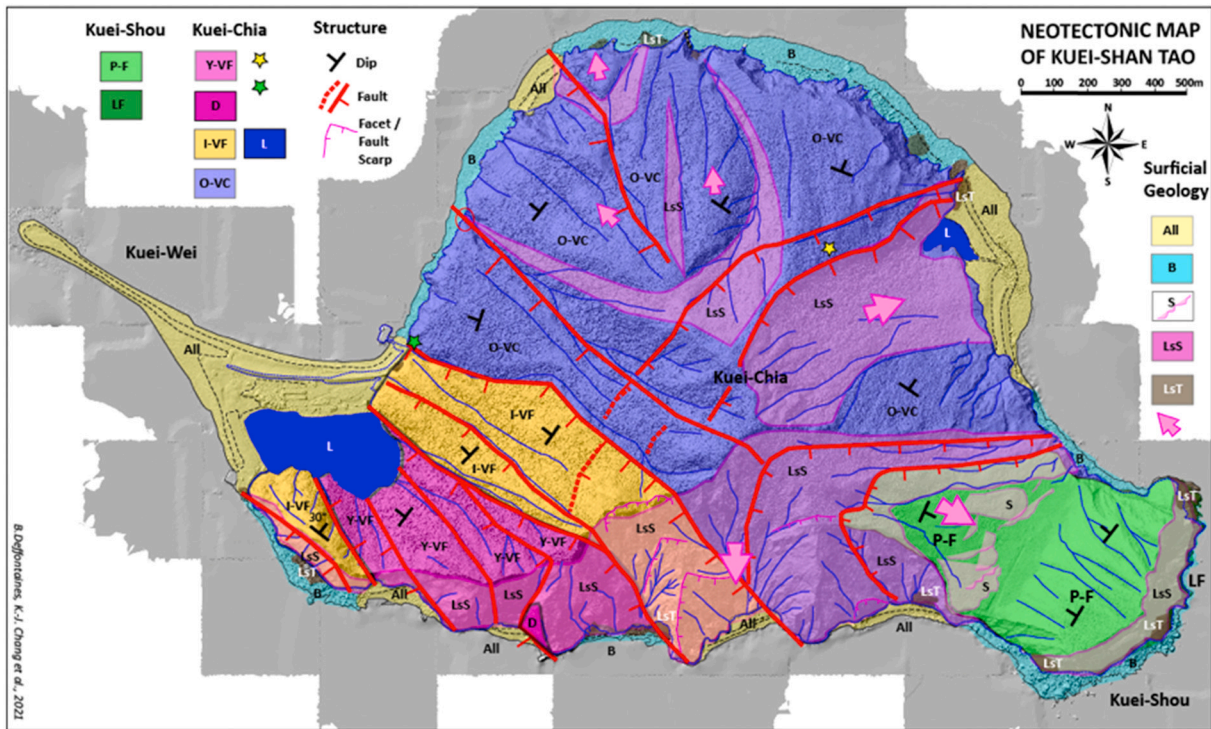


**Fig. 9.** Kuei-Shan Tao Neotectonic map: Kuei-Shou: P—F Pyroclastic Fall (cover the top), LF: Massive Lava-Flow (at the eastern base); Kuei-Chia: Y-VF: Younger volcanic fissural facies; D: vertical Dyke; I-VF = Intermediate in age Volcanic fissural facies; O-VC: Older volcanic cone facies. L: Lake; Yellow star: cores A & B sites; Green star: Dating site [Chen et al. \(2001\)](#). Surficial geology: All: Thinner small boulders, gravel, & sand shoreface marine deposits; B: Boulders and Coarser shoreface marine deposits; S: Solifluction processes reactivating the Kuei-Shou Pyroclastic-fall; LsS: Landslide and Fault Scarps; LsT: Landslide toe (accumulation of fallen materials to be removed by sea curenrs, waves, & tides actions), Large purple arrows highlight the downstream displacements of the lithologies. One may notice the two set of perpendicular faults that offset the KST volcanic island.

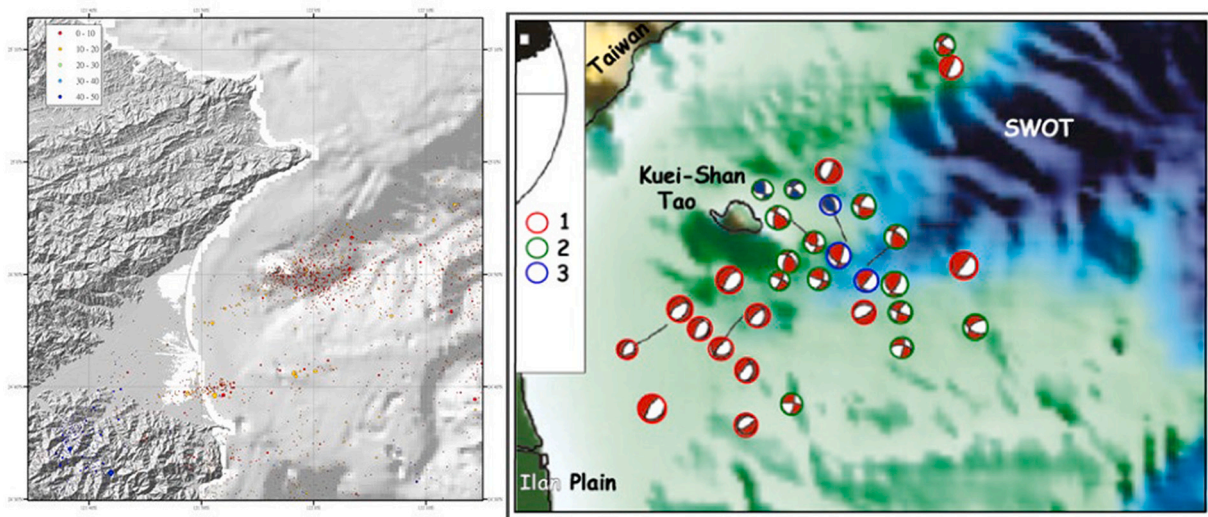


**Fig. 10.** Seismicity around Kuei-Shan Tao. Fig. 10 left: Epicenters of shallow earthquakes depth 0 to 50 km, see the two clusters located East and south of KST - source: [http://seismology.gi.ntu.edu.tw/download.htm?fbclid=IwAR0ncf1jPLt1JaAeE58\\_JBwsa0YDcsJ0A0AQwJb4GORZEN3Cs2wGLnO5UNI](http://seismology.gi.ntu.edu.tw/download.htm?fbclid=IwAR0ncf1jPLt1JaAeE58_JBwsa0YDcsJ0A0AQwJb4GORZEN3Cs2wGLnO5UNI). Fig. 10 right: Focal mechanism of larger Earthquakes, modified from Konstantinou et al. (2013, their Fig. 12, p. 31). 1: Normal focal mechanism; 2: Strike-slip focal mechanism; 3: Compressive focal mechanism. All those focal mechanisms, the 3 directions of the stress axes are the same. There are only permutations in the magnitudes (herein  $\sigma_3$  is NW-SE for the normal and the strike-slip state of stress, there is just a permutation of  $\sigma_1 / \sigma_2$ :  $\sigma_1$  vertical for Normal focal mechanism) to  $\sigma_1$  horizontal (Strike-Slip focal mechanisms).

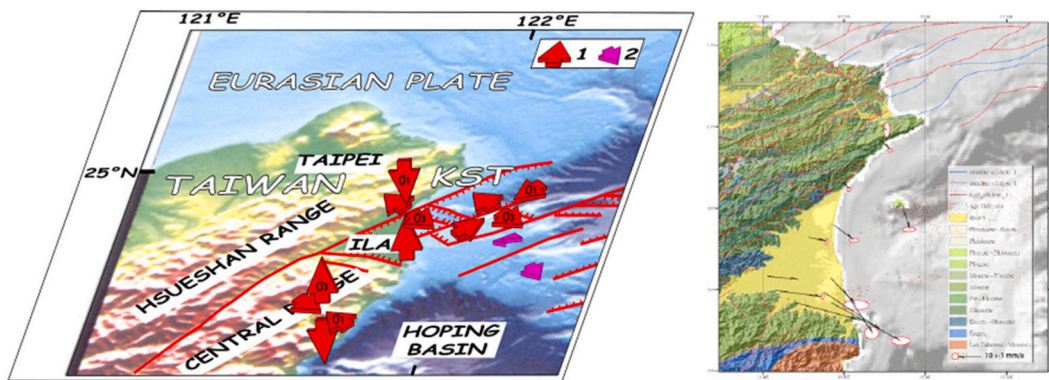


**Fig. 11.** left: State of stress deduced from the earthquake focal mechanisms. Red lines: major faults (modified from Deffontaines et al., 2001); 1: Red arrows: location of the major state of stress in NE Taiwan & Kuei-Shan Tao (modified from Konstantinou et al., 2013); 2: Purple arrows: deduced relative displacements due to the active tectonic set of faults recognized herein. Three states of stress with unchanged directions but with magnitude permutations: from compressive (NE Taiwan collision), Extensive (Ilan plain), to strike-slip regime (East of KST). Only permutations prevail. Fig. 11 right: GPS motions around Kuei-Shan Tao (Eurasia fixed). One may note the absolute SSE centimetric/year average KST displacement which is situated in between the low motion of the Hsueshan shoreline (NE Ilan Plain) and the contrasting higher GPS displacements of the southeast Ilan Plain.

volcanic dykes and highly dipping normal faults. Despite we miss their different ages, we distinguish in the SW KST, two other strips of volcanic rocks NW-SE trending corresponding to the previous Kuei-Chia volcanic apron (older strata) offset by vertical NW-SE dykes and faults (the so-called intermediate in age Volcanic Fissural (IVF in yellow) and in red the Younger volcanic fissural facies (OVF). Their tectonic attitude corresponds to a « graben-like » geometry and their relative ages is only proposed from their altitude and the lava geometries in the field (see Fig. 8 - quadrangle 5 bottom left). It is definitely needed to do much more datings in the near future to precise their ages.

6.2. Structure

Kuei-Chia corresponds to a volcanic cone affected by large faults that crosses the island. They are visible on its northeastern and its southwestern sides. The northeastern part is affected by NE-SW faults with a normal component reactivating a dissymmetric rotational landslide (see

Chiu et al., 2010; Huang et al., 2021). The southwestern part is faulted by numerous WNW-ESE trending major vertical faults differentiating blocks dipping generally to the NW. It gives a horst-graben-like structural geometry that fits with the basin structures of the SWOT offshore. The SW part is also intersected by numerous vertical NW-SE dykes seen on the UAS-DSM, the orthophotos and in the fields (observations from a boat). Consequently, Kuei-Shan Tao reveals two very contrasting volcanic and tectonic setting: the setting of a volcanic cone then its fractured by two fault sets NE-SW and WNW-ESE trending. At least, the « bayonet » geometry of the southern shoreline highlights the interaction of these two perpendicular fault sets which explains also the weathering of the Kuei-Chia southern flank. The discussion below will precise this aspect.

6.3. Erosion processes in the KST evolution

The strong Kuroshio Sea currents (one of the strongest in the world)

erode actively the KST shoreline removing any fallen materials and blocks. Moreover, the large fault zones are heavily weathered and altered that favor landsliding processes. Kuei-Chia made of volcanic series containing massive lava flow is harder to erode contrasting to the younger in age Kuei-Shou Pyroclastic edifice which is easily eroded by sea currents, sea waves and tides actions. With the precise UAS-DSM we may reconstruct the geometry of lava flows by interpolating offshore data and onshore outcrops geometry and consequently propose an erosion rate for the construction of marine terraces under the Kuro-Shio Sea currents environment (P. Huang et al. work in progress).

## 7. Discussion: the Kuei-Shan Tao geological mapping implications on geodynamics and neotectonics

If we want to better understand the transition in between the Taiwan collision and the opening of the southwest Okinawa Trough, several key arguments should be added and discussed in regards to the updated KST geological mapping.

### 7.1. Kuei-Shan Tao andesite datings (Chen et al., 2001)

Some geochronological datings had been acquired on the NE Taiwan volcanic island with various methodologies. For instance, [Juang and Chen \(1989\)](#) dated the KST andesite by K—Ar method, they found an age of  $20 \pm 10$  ka BP. Then, [Chen et al. \(1993\)](#) using U—Th method dated pumices « in the Okinawa Trough » and revealed three major eruptions dated 10, 30 and 70 ka BP. The problem is that for these two publications we miss the sample locations.

More recently [Chen et al. \(1998, 2001\)](#) dated with a thermoluminescence method a heated sedimentary siltstone xenolith embraced within the underlying massive andesite ( $7 \pm 0,7$  ka BP so Holocene in age). If [Chen et al., 1998, 2001](#) miss their sampling location, [Chiu et al. \(2010\)](#) propose their inferred location East of the KST wharf. But following the [Chen et al. \(2001\)](#) description, the sampling location should correspond to the massive « LF5 » lava flow whereas [Chiu et al. \(2010\)](#) locate the sampling site (green star see their [Fig. 4](#)) in the pyroclastic flow « PF5 » which does not match really. This sampling location is important as it is the unique reliable and precise existing KST Lava Flow dating.

This dating is important for at least two reasons: (1) It gives the ages of the latest Lava-Flow of conic geometry of the Kuei-Chia volcano as it is one of the summital and latest lava flow succession getting out of the Kuei-Chia caldera, on one hand. So this age gives an approximate dating when was the jump in the structural geometry: from a cone-like to a NW-SE graben-like geometry; on the other hand (2) Kuei-Shou («head of the turtle» eroded pumice volcano situated at the eastern tip of KST) is overlying the same lava flow volcanic strata (as already observed by [Hsu, 1963](#); and [Chiu et al., 2010](#)). It means that Kuei-Shou is younger than this  $7 \pm 0,7$  ka age. One may realise also that the Pyroclastic deposits PF of [Chiu et al. \(2010\)](#) that overly the whole island may be linked to both Kuei-Chia and then Kuei-Shou volcanic activities. It is consequently important to date different Lava Flows especially in the SW part of the island if possible, in the near future. Due to the recent age, [Chen et al. \(2001\)](#) conclude that KST is an active volcano and may be submitted to future eruptions.

### 7.2. Seismicity (Konstantinou et al., 2013)

The Ilan Plain and the SWOT area (all around KST) is submitted to an intense shallow earthquake activity (EQ below). ([Fig. 10A](#), <http://seismology.gln.ntu.edu.tw/download.htm?fbclid=IwAR0ncf1jPLt1JaAeE58JBwsa0YDcsJ0A0AqWJb4GORZEN3Cs2wGLnO5UNI> - shallow EQ, magnitudes (>2), monitored from 1990 to 2016). We notice two clusters of earthquake epicenters offshore the Ilan plain. Numerous previous authors studied the earthquake focal mechanisms of NE Taiwan (e.g. [Tsai et al., 1975, 1977, 1981](#); [Yeh et al., 1989](#); [Yeh et al., 1991](#) / [Fig. 4](#);

[Kao et al., 1998](#) / [Fig. 2a](#); [Ku et al., 2009](#)) / [Fig. 2](#); [Lai et al., 2009](#), [Fig. 2](#); [Wu et al., 2009](#) / [Fig. 4](#); [Huang et al., 2012](#) / [Fig. 4](#); [Konstantinou et al., 2013](#) / [Fig. 12](#), [Kang et al., 2015](#) / [Fig. 2](#)). All their results are compatible with a NW-SE extension all around Kuei-Shan Tao. In order to characterize the state of stress, we re-analysed herein also the focal mechanisms of the 31 earthquakes (max Magnitude 4.4 and with a depth shallower than 30 km) acquired with a local temporary network from January to December 2008 by the Institute of Earth Sciences (Academia Sinica, cf. [Konstantinou et al., 2013](#), see [Fig. 10](#) right). ([Konstantinou et al., 2013](#)) settled a local seismic network active during one year (2008). 425 monitored shallow earthquakes (depth ranging from 2.5 to 10 km), 31 focal mechanisms were calculated ([Fig. 10](#) right). If we re-analyse these focal mechanisms from a tectonic point of view, we notice two major clusters of EQ on the eastern and southern part of KST characterized two major sets of contemporaneous state of stress:

- (1) A cluster of earthquakes is located E and SE close to KST (see [Fig. 10A & B](#)). Already recognized by [Huang et al. \(2012\)](#), who noted its position, depth shallower than 15 km and magnitudes larger than 3.5. [Konstantinou et al. \(2013\)](#) process Strike-slip focal mechanisms (15 green circles, [Fig. 10](#) right) are gathered and located East of Kuei-Shan Tao. They reveal a general state of stress with  $\sigma_2$  vertical and both NE-SW  $\sigma_1$ , and NW-SE  $\sigma_3$  horizontal axes.
- (2) Numerous earthquake focal mechanisms highlighting a state of stress of normal faults (13 red circles, [Fig. 10](#) right) with  $\sigma_1$  close to the vertical and slightly tilted generally to the SE whereas both horizontal component  $\sigma_3$  trends NW-SE and  $\sigma_2$  is trending NE-SW. Those normal focal mechanisms are gathered generally south of KST. This direction of stress tensor is coherent with the initial NW-SE regional trending of the SWOT structures ([Sibuet et al., 1998](#); [Fabbri and Fournier, 1999](#); [Deffontaines et al., 2001](#); [Sibuet et al., 2002](#)). This normal state of stress is compatible with the NE-SW set of faults that we recognized onshore the eastern flank of Kuei-Chia geological mapping and should correspond to the settling of Kuei-Shou (East of the island) pyroclastic falls volcanic cone. It might be associated with the activation/re-activation of the major landslide situated to the northeast of Kuei-Chia ([Hsu, 1963](#); [Chiu et al., 2010](#); [Huang et al., 2021](#)).
- (3) Very few compressive earthquake focal mechanisms (only three (3), see blue circles of [Fig. 10B](#)) can be seen in one year monitoring time period (horizontal component:  $\sigma_1$  trending ENE-WSW, and  $\sigma_2$  slightly tilted trending NNW-SSE, whereas  $\sigma_3$  is almost vertical and slightly tilted to the north. They are also grouped close to the east of KST. This « compressive » state of stress oblique to the inferred structures in that area is more difficult to understand. As we observed already, all these focal mechanisms have the same axes directions for the stress axes. This compressive state of stress is anyway a bit surprising, as we did not recognize in the KST outcrops NW-SE trending thrusts. We just notice the vertical and highly dipping faults, and some reverse drag-folds along normal faults in the northern KST shoreline that may be interpreted as due to tectonic inversion ([Fig. 7F](#) and [7G](#)) and should be confirmed by more field work in the near future.
- (4) At last, SW of KST, we wait for a direction of extension compatible with the settings of the NW-SE volcanic dykes and the associated WNW-ESE graben-like faults (see the neotectonic map of KST). In contrast, all the numerous normal focal mechanisms reveal  $\sigma_3$  WNW-ESE trending, so perpendicular to the inferred structural horst and graben geometry! We see different possible explanation: either the stress trajectories should turn at the SWOT tip, or the monitoring time period is too short to get the whole set of deformation and the whole seismic cycles of the place.

So, in between these 31 focal mechanisms, we just note permutations in the magnitudes of the state of stress (e.g.: strike-slip and compressive state of stress have the same axes directions with only a vertical/horizontal permutation of the  $\sigma_1/\sigma_3$  stress axes,  $\sigma_2$  is unchanged NNW-SSE trending). If we look closely, we could notice that all the axes of those focal mechanisms are not exactly horizontal & vertical but slightly tilted which is in favor of the re-activation of previous faults and structures. Consequently, both nodal planes of the normal focal mechanisms are almost vertical and horizontal which favor either the settings of active vertical tension joints ENE-WSW (which are perpendicular to the dykes observed herein south of KST), or the settings of active sills filled by lava within the southern offshore graben. The large lateral extension of the « normal » focal mechanisms location may be in favor of this assumption.

The presence of graben-like structures NW-SE trending situated onshore and offshore situated on both side of KST, added with both high normal and strike-slip earthquake activities with their associated tectonic regime are in favor of a large « pull-apart » geometry guided by the transtensional right lateral ENE-WSW faults that correspond to the offshore extension of the Lishan fault (Lee et al., 1997). KST appears to be in the middle of this “pull-apart basin geometry” dividing in two active grabens NW-SE trending situated northeast and southwest of KST. The two KST directions of faults WNW-ESE and NE-SW faults (Fig. 11 left) are fully compatible with this large pull-apart structural geometry. The relative displacements (purple arrows) is supported by the absolute GPS measurements with an Eurasian reference frame (Fig. 12) where KST is moving with an average displacement of several centimetre/year to the SSE (see Yu and Tsai, 1979; Yu and Lee, 1986; Yu et al., 1997; Rau et al. (2008, Fig. 2), Angelier et al. (2008); Industrial Technology Research Institute – Central Geological Survey, 2013, ...). One may notice the much higher magnitudes of the absolute displacements to the SE of the northeastern tip of the Central Range (see south of the Ilan Plain, Fig. 12), and the much smaller displacements of the Hsueshan Range along the NE-SW shoreline facing the northern flank of KST.

The strike-slip state of stress with the horizontal  $\sigma_3$  (NW-SE) is fully compatible with the SE extension of the Ryu-Kyu accretionary prism GPS displacement (southern boundary of the SWOT, see Fig. 11 right).

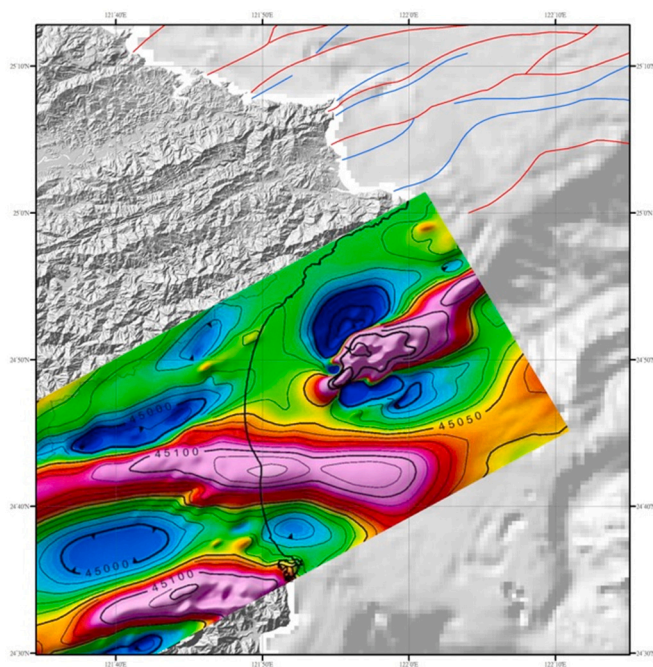


Fig. 12. Ilan Plain and SWOT aeromagnetic survey (modified from Industrial Technology Research Institute – Central Geological Survey, 2013). One may notice the magnetic positive anomalies that correspond to the earthquake clusters (Fig. 10 left and right).

### 7.3. Aeromagnetic survey, volcanic activity and earthquake clusters

Interesting findings, a detailed aeromagnetic survey along the southwestern tip of the Okinawa Trough and the Ilan Plain (NE Taiwan see Fig. 12 modified from Tong et al., 2013a, 2013b, Industrial Technology Research Institute - CGS, 2013) had been shot by the Central Geological Survey (see Industrial Technology Research Institute – Central Geological Survey (2013)). The major magnetic positive anomalies correspond to the two earthquake clusters described above. KST is situated at the western tip of the northern positive magnetic anomaly that should correspond to the KST volcanic chamber at depth. This positive magnetic anomaly is ENE-WSW trending which is compatible with the NW-SE extension already recognized by the focal mechanisms of earthquakes (NW-SE trending  $\sigma_3$ ).

Moreover there is very high heat flow value around KST (Chiang et al., 2010) and the island is bounded to the east and the south by numerous offshore fumarolles (Marumo and Hattori, 1999; Kuo, 2001; Lee, 2005; Yang et al., 2005; Zeng et al., 2007; Chen et al., 2018; Huang et al., 2021). These fumarolles should correspond to the different fault outcropping above this positive magnetic anomaly.

The second positive major magnetic anomaly is E-W trending and extend from the Lishan fault onshore crossing the Ilan Plain and extends to offshore above the Ilan ridge. Its geometry is much simpler and corresponds to the settling of E-W dykes (Lai et al., 2009). It should be the signature of the beginning of the NW-SE extension. It ends abruptly eastward offshore but the aeromag survey should be extended further southeast.

### 7.4. Landslide activities and reactivation

As 0.45 millions of inhabitants are living in the flat lying Ilan Plain, situated in front of KST, it is an important issue to characterize the landslides motion: may they be tsunamogene (or not)? Pichun Huang et al., 2021 taking into account sparker seismic profiles north of Kuei-Chia offshore study the seismic signature of the landslide (see Huang et al., 2021).

### 7.5. KST volcanic settings

In the light of all previous arguments, we propose the following scenario for the Kuei-Shan Tao volcanic evolution.

First, the Kuei-Chia volcanic cone geometry had been constructed through numerous eruptions consisting of alternance of Lava Flows and Pyroclastic falls with a summit caldera (Fig. 13A). Then later, the Kuei-Chia volcanic cone was progressively fractured and dismantling by two sets of normal faults that should be still tectonically and volcanically active: (1) one is WNW-ESE situated to the southwest of the Kuei-Chia edifice, and (2) the NE-SW trending situated east of Kuei-Chia and who is responsible of the settling of Kuei-Shou and responsible of the destruction of the caldera (Fig. 13B and Fig. 13C). These two sets of normal faults evoke a “rhomboidal-like” geometry which in tectonic studies is usually associated with a “pull apart” geometry dominated by the right lateral NE-SW faults that should correspond to an eastward offshore extension of a branch of the Lishan Fault (see Fig. 11left). But one may bear in mind, that this “rhomboidal-like” structural geometry of these two sets of normal faults may also be explained by two sets of perpendicular NW-SE and NE-SW extensions (but we miss the NE-SW extension presently!).

As a consequence, if this dismantling of the Kuei-Chia volcanic cone is confirmed, the NW-SE graben like structures offshore southwest of Kuei-Chia will be reactivated in the near future. This is documented by the following arguments: (1) the location of the epicenters of shallow earthquakes are located offshore east and south of KST (Fig. 10 left and right), (2) the focal mechanisms of larger earthquakes are also situated offshore east and south of KST (Fig. 10 right), (3) the present position of the positive magnetic anomaly associated with the KST magmatic

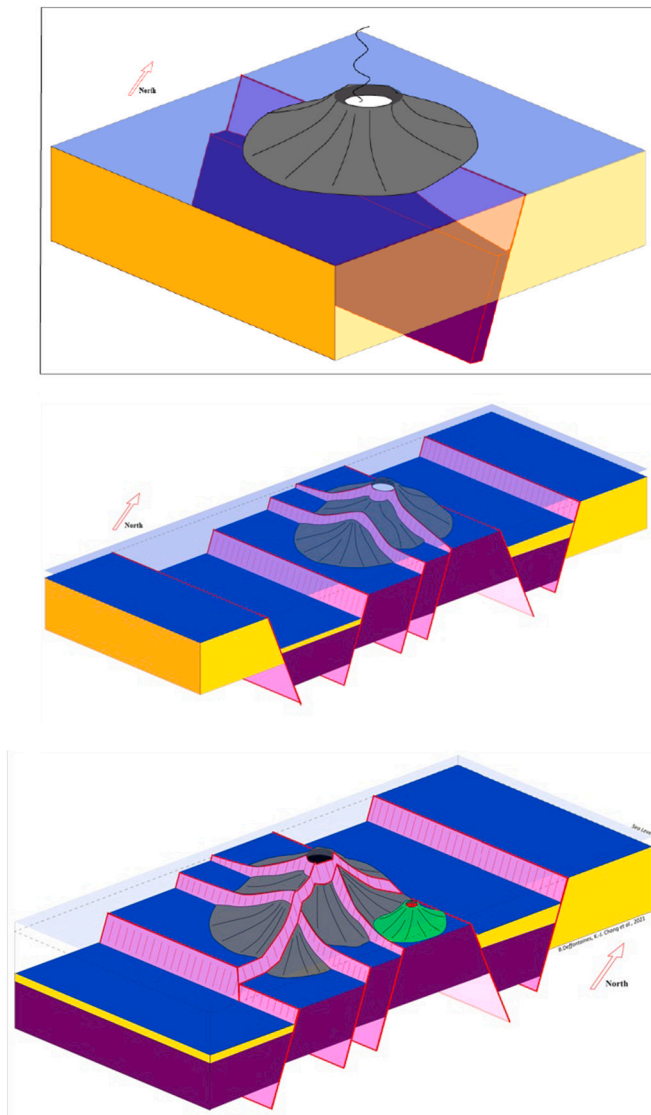


**Fig. 13.** Evolution of Kuei-Shan Tao volcanic island. **Fig. 13A** (top): Initial Kuei-Chia with a volcanic « cone-like » geometry with the NW-SE settings of dykes under a transtensional right-lateral strike-slip tectonic regime; **Fig. 13B**: Progressive dismantling of the Kuei-Chia volcanic cone (post 7 ka) with a WNW-ESE « graben-like » geometry developing offshore SW KST. **Fig. 13C**: (bottom): setting of Kuei-Shou (in light green) above the latest volcanic Kuei-Chia volcanic cone activity. Red areas: Fault planes; Purple: massive lava flow, Yellow: sediment deposits.

chamber is situated east of KST and beneath Kuei-Shou; and (4) the important fracturing of the two sets of normal faults should favor lava flows in the near future either east of Kuei-Chia (around Kuei-Shou) or offshore in the graben-like structure south of Kuei-Chia.

Taking into account the KST neotectonic map, and to summarize (Fig. 13A, 13B and 13C), all these structural arguments are in favor of the edification of an initial Kuei-Chia volcanic cone geometry with a summit caldera, due to extensive tectonic regime(s) (O-VC, see Fig. 9). Then it is followed by both (1) the NW-SE normal faults that create the set of horst and grabens southwest of Kuei-Chia (I-VF & Y-VF of Fig. 9) and which are associated with vertical dykes (outcropping in the southern KST shoreline); and (2) the NE-SW normal faults on which is settle Kuei-Shou. There is fluids percolations and mineralisation occur along those fault zones with numerous fumaroles along the shoreline and offshore.

## 7.6. Geodynamic implications

Since decades, many authors discussed about the relations in between the NW-SE and the N-S extension in the SWOT (Kimura, 1985; Letouzey and Kimura, 1986; Sibuet et al., 1995, 1998; Wang et al., 1999; Fabbri and Fournier, 1999...). We show on KST that two sets of normal faults prevail already in the early stage of the opening of the SWOT back-arc basin which are associated with the volcanic and tectonic activities. The structural geometry of KST volcano reveal the simultaneity of these two perpendicular sets of normal faults. Consequently, we propose herein a right lateral pull-apart structural geometry along the NE-SW sets of major transtensional faults for the progressive opening of the SWOT which may be slightly different than the proposed clockwise rotation of  $25^\circ$  of the Ryukyu arc given by Fabbri and Fournier (1999). Following our assumptions, the Ilan ridge/Ryukyu arc should correspond to the progressive dismantling of the northern tip of the Taiwan Central Range (Shyu et al., 2005). If it is so, it has geodynamic impacts on the geology of Japanese islands.

Further studies should focus on the quantification of the displacements for instance using the Interferometric point of view in order to quantify the line of sight (LOS) component. As a perspective point of view, it is now a key issue to much better estimate the earthquake cycles in order to distinguish the creeping and earthquake components on this active volcanic tectonised area.

## 7.7. Limit and uncertainties of a morphostructural study

Morphostructural interpretations (interpretations from the topography, from aerial photographs or satellite images, from slides or field-photographs...) always face the same criticisms from readers: « where are the field evidences »; where are the « solid data » that may confirm your views?; where are the « uncertainties »? what are the alternatives possible morphostructural interpretations?

Of course, any results need to be validated in « some ways and to some degree ». In geology both the volcanic environment as well as the muddy/clayey/turbiditic environments are difficult to study in the fields from the structural point of view for different reasons (Deffontaines et al., 2018, 2019 and see the introduction above). Morphostructural analysis with a pluricentimetric digital topography is a good (unique?) preliminary approach in such active environment to reach a comprehensive reliable structural scheme. This KST study where numerous geological mappings had been done in the fields by good geologists (Ichikawa in the 1930s, Hsu L.C., in the 1960's and more recently Chiu et al. (2010) geologists of the Central Geological Survey did not provide any structural scheme of this area despite its high earthquake seismic activity. Only our detailed morphostructural analysis propose a documented structural scheme of this area. It will surely be discussed, questioned, and/or refined in the future and a new and more convincing structural scheme will then be established on the basis of previous works.

## 8. Conclusions

We have updated the geological mapping of the andesitic Kuei-Shan Tao volcanic island (northeastern Taiwan and southwestern tip of the Okinawa Trough) taking into account our new High Resolution UAS Digital Surface Model (7.5 cm ground resolution) combined to the pre-existing published geological maps. Using morphostructural principles, we revealed the locations of two major sets of normal faults (WNW-ESE and NE-SW trending) that offset the Kuei-Chia volcanic cone. We precise the location of the previous caldera and the geometry of two major landslides situated in northern Kuei-Chia. We propose also a KST structural sketch map that helped us to reconstruct the recent volcanic and tectonic history. Kuei-Chia is a simple volcanic conic fractured by both active WNW-ESE and NE-SW trending highly dipping normal faults. Those sets of normal faults should behaved as younger as it affects

the last higher lava flows (LF5 and LF6 of Chiu et al., 2010) which are associated locally with vertical volcanic dykes that are inferred to be local KST feeders. These dykes had been filled with andesitic lava flow and are still standing above the southern shoreline. The thermoluminescence age (TL) of  $7 \pm 0.7$  ka that date the major northern KST volcanic lava flow give a major constraint to the transition in between the two volcanic geometries: from the « cone-like » to the « graben-like » geometries.

The two earthquakes' clusters are situated above magmatic chambers. The focal mechanisms studied herein highlight both the NW-SE extension and the strike-slip regimes (with  $\sigma_1$  NE-SW) that reactivate conjugate sets of WNW-ESE and NE-SW highly dipping normal faults. We propose that KST island is situated in a large "right lateral NE-SW transtensive pull-apart".

From the geodynamic point of view, Kuei-Shan Tao is the unique outcropping area that gives some tectonic arguments to the transition in between the NW-SE compressive tectonic regime prevailing in the Taiwan collision and the N-S extension of the southwest Okinawa Trough.

The KST earthquake cycle and their associated volcanic hazard has a special importance for the local citizens due to the presence of numerous earthquakes and the existing KST landslide activity situated on both sides of the island. Some studies focus on the landslide affecting the northern side of KST facing the densely populated flat lying Ilan plain as well as the sensitive industrial infrastructures such as the Gongliao nuclear power plant situated NE of Taiwan. Moreover, one may consider the importance to monitor any active volcanic island situated around northern Taiwan in order to prevent volcanic eruptions.

#### Credit author statement

Conceptualization, B.D., K.-J.C., P.-H., S.K. H.; methodology, B.D., K.-J.C., P.H., S.K. H., C.-S. L.; investigation, B.D., K.-J.C., P.H., S.K. H.; writing: all; editing: all

#### Declaration of Competing Interest

The authors declare no conflict of interest.

#### Acknowledgements

Authors would like to thank reviewers for their constructive remarks. B. Deffontaines would like to thank his family for most of the funding of his scientific research since 2008 (without fundings of its UPEM-UGE institution). Special thanks to the CNRS through the International Research Project CNRS-MOST France Taiwan G2E, now in the Chair: Frédéric Mouthereau (Pr Univ. Toulouse) and Gueorgi Ratzov (Univ. Nice) in the French side, and Ya-Ju Hsu (Academia Sinica) and Jin-Yi Lin (National Central University) for the Taiwanese side. Special thanks to Jacques Angelier (UPMC), Serge Lallemand (Univ. Montpellier), Lionel Siame (CEREGE), Char-Shine Liu (IONTU-NTU), Hsu Shu-Kun (NCU) and Jian-Cheng Lee (IES, Academia Sinica) who chaired the previous Laboratoire International Associé ADEPT, then D3E, N°536 CNRS/MOST France-Taiwan. This project was partially supported from the Ministry of Science and Technology, MOST 109-2116-M-027-003 and MOST 110-2116-M-027-003

#### References

Angelier, J., Chang, T.-Y., Hu, J.-C., Chang, C.-P., Siame, L., Lee, J.-C., Deffontaines, B., Chu, H.-T., Lu, C.-Y., 2008. Does extrusion occur at both tips of the Taiwan collision belt, Insights from active deformation studies in the Ilan Plain and Pingtung Plain regions. *Tectonophysics* 466, 356–376.

Chang, K.J., Chan, Y.C., Chen, R.F., Hsieh, Y.C., 2018. Geomorphological evolution of landslides near an active normal fault in northern Taiwan, as revealed by LiDAR and unmanned aircraft system data. *Nat. Hazards Earth Syst. Sci.* 18, 709–727.

Chen, L.R., Zhuai, S.K., Shen, S.X., 1993. Isotopic characteristics and age determination of pumices from Okinawa Trough. *Sci. China* 23 (3), 324–329 (in Chinese).

Chen, Y.-G., Wu, W.-S., Liu, T.-K., Chen, C.-H., 1998. A Holocene volcanic island: Kuei-Shan Tao. In: *Annu. Meet. Geol. Soc. China, Prog. Abstr.*, pp. 104–105.

Chen, Y.-G., Wu, W.-S., Chen, C.-H., Liu, T.-K., 2001. A date for volcanic eruption inferred from a siltstone xenolith. *Quat. Sci. Rev.* 20, 869–873.

Chen, X.-G., Lyu, S.-S., Zhang, P.-P., Yu, M.-Z., Chen, C.-T.A., Chen, Y.-J., Li, X., Jin, A., Zhang, H.-Y., Duan, W., Ye, Y., 2018. Gas discharges from the Kueishantao hydrothermal vents, offshore Northeast Taiwan: Implications for drastic variations of magmatic/hydrothermal activities. *J. Volcanol. Geotherm. Res.* 353, 1–10.

Chiang, H.-T., Shyu, C.-T., Chang, H.-L., Tsao, S., Chen, C.-X., 2010. Geothermal monitoring of Kueishantao island offshore of northeastern Taiwan. *Terr. Atmos. Ocean. Sci.* 21, 563–573. [https://doi.org/10.3319/TAO.2009.11.02.01\(TH\)](https://doi.org/10.3319/TAO.2009.11.02.01(TH)).

Chiu, C.-L., Song, S.-R., Hsieh, Y.-C., Chen, C.-X., 2010. Volcanic characteristics of Kueishantao in Northeast Taiwan and their implications. *Terr. Atmos. Ocean. Sci.* 21 (3), 575–585. [https://doi.org/10.3319/TAO.2010.02.22.02\(TH\)](https://doi.org/10.3319/TAO.2010.02.22.02(TH)).

Clift, P.D., Lin, A.T.S., Carter, A., Wu, F., Draut, A.E., Lai, T.-H., Fei, L.-Y., Schouten, H., Teng, L., 2008. Post-collisional collapse in the wake of migrating arc-continent collision in the Ilan Basin, Taiwan, Chapter 12 The Geol. Soc. of America. In: Draut, A.E., Clift, P.D., Scholl, D.W. (Eds.), *Special Paper 436: Formation and Applications of the Sedimentary Record in Arc Collision Zones*, pp. 257–278. [https://doi.org/10.1130/2008.2436\(12\)](https://doi.org/10.1130/2008.2436(12)).

Dauteuil, O., Bergerat, F., 2005. Interactions between magmatism and tectonics in Iceland: a review. *Geodin. Acta* 18/1, 1–9.

Deffontaines, B., 1985. Proposition d'une méthode géomorphologique permettant une approche de la néotectonique en pays tempéré, exemple d'application: la région de Fougères (France), Rapport Interne BRGM, 85SGN659GEO, 107 p. + Annexes.

Deffontaines, B., 1991. Développement d'une méthodologie d'analyse morphostructurale et morphonéotectonique; Analyse des surfaces enveloppes, du réseau hydrographique et des modèles numériques de terrain; Applications au Nord-Est de la France, (Thèse de Géologie structurale et de Télédétection, Univ. Paris VI, N°90–6). Rapport Interne BRGM N°32005, 194p. + Annexe.

Deffontaines, B., 2000. Formes et déformations de la surface terrestre : Approches morphométriques et applications, Habilitation à Diriger des Recherches. Univ. Pierre Marie Curie P6, 60p. + Annexes.

Deffontaines, B., Chorowicz, J., 1991. Principles of drainage basin analysis from multisource data, application to the structural analysis of the Zaire Basin. *Tectonophysics* 194, 237–263. [https://doi.org/10.1016/0040-1951\(91\)90263-R](https://doi.org/10.1016/0040-1951(91)90263-R). ISBN: 0040-1951.

Deffontaines, B., Chotin, P., Ait Ibrahim, L., Rozanov, M., 1992a. Investigation of active faults in Morocco using morphometric methods and drainage pattern analysis. *Geol. Rundsch.* Stuttgart 81 (1), 199–210. <https://doi.org/10.1007/BF01764549>.

Deffontaines, B., Cadet, J.P., Fourniguet, J., 1992b. L'analyse des surfaces enveloppes appliquée à l'étude morpho-structurale de l'Est de la France. *Geodinamica Acta Paris* 5 (4), 279–292. <https://doi.org/10.1080/09853111.1992.11105233>.

Deffontaines, B., Pubellier, M., Rangin, C., Quebral, R., 1993. Discovery of an Intra-arc transform zone in Mindanao (Philippines) using morphotectonic data, *Zeitschrift für Geomorphologie, Berlin - Stuttgart., Suppl.-Bd.* 94, pp. 261–273. ISSN : 0044-2798 – INIST-CNRS (Francis) : 6443045.

Deffontaines, B., Lee, J.C., Angelier, J., Carvalho, J., Rudant, J.P., 1994. New geomorphic data on Taiwan active orogen: a multisource approach. *J. Geophys. Res.* 99 (B8), 20,243–20,266. <https://doi.org/10.1029/94JB00733>. ISBN: 2156-2202.

Deffontaines, B., Liu, C.-S., Angelier, J., Lee, C.-T., Sibuet, J.-C., Tsai, Y.-B., Lallemand, S., Lu, C.-Y., Lee, C.-S., Hsu, S.-K., Chu, H.-T., Lee, J.-C., Pathier, E., Chen, R.-F., Cheng, C.-T., Liao, C.-W., Lin, C.-C., Hsu, H.-H., 2001. Preliminary neotectonic map of onshore-offshore Taiwan. *Terr. Atmos. Ocean. Sci.* 2001, 339–349. Sup. Issue, May.

Deffontaines, B., Liu, C.-S., Hsu, H.-H., 2016. Structure and deformation of the southern Taiwan accretionary prism: the active submarine Fanglei Fault Zone offshore west Hengchun Peninsula. *Tectonophysics* 692, 227–240. <https://doi.org/10.1016/j.tecto.2016.11.007>.

Deffontaines, B., Chang, K.-J., Champenois, J., Fruneau, B., Pathier, E., Hu, J.-C., Lu, S.-T., Liu, Y.-C., 2017. Active interseismic shallow deformation of the Pingting terraces (Longitudinal Valley – Eastern Taiwan) from UAV high-resolution topographic data combined with InSAR time series. *Geomat. Nat. Hazards Risk* 8, 120–136. <https://doi.org/10.1080/19475705.2016.1181678>.

Deffontaines, B., Chang, K.-J., Champenois, J., Lin, K.-C., Lee, C.-T., Chen, R.-F., Hu, J.-C., Magalhaes, S., 2018. Active tectonics of the onshore Hengchun Fault using UAS DSM combined with ALOS PS-InSAR time series (southern Taiwan) (discussion paper, 10.5194/nhess-2017-55). *Nat. Hazards Earth Syst. Sci.* 18, 829–845. <https://doi.org/10.5194/nhess-18-829-2018>.

Deffontaines, B., Chang, Kuo-Jen, Lee, Chyi-Tyi, Magalhaes, Samuel, Serries, Gregory, 2019. Neotectonics of the southern Hengchun Peninsula (Taiwan): Inputs from high resolution UAS Digital Terrain Model, updated geological mapping and PSInSAR techniques. *Tectonophysics* 767, 128–149. <https://doi.org/10.1016/j.tecto.2019.06.019>. EGU 2018, Lacombe O. Ed.

Fabbri, O., Fournier, M., 1999. Extension in the southern Ryukyu arc (Japan): link with oblique subduction and back arc rifting. *Tectonics* 18 (3), 486–497.

Ho, C., 1986. A synthesis of the geologic evolution of Taiwan. *Tectonophysics* 125, 1–16.

Hsu, L.-C., 1963. Petrology of the Pleistocene andesite from Kueishantao, northern Taiwan. *Acta Geol. Taiwan. In: Science Report of the National Taiwan University*, vol. 10, pp. 29–40, 4 Fig, 3 tables, 3 plates.

Hsu, L.-C., Ku, C.C., 1962. Geology and mineral deposits at Kuei-Sha Tao, Ilan. In: *Ann. Rep. Mineral Survey Team, MOEA 1961–1962*, pp. 267–280.

Hsu, S.-K., Sibuet, J.-C., Monti, S., Shyu, C.-T., Liu, C.-S., 1996a. Transition between the Okinawa Trough backarc extension and the Taiwan collision: new insights on the southernmost Ryukyu subduction zone. *Mar. Geophys. Res.* 18, 163–187.

- Hsu, S.-K., Sibuet, J.-C., Shyu, C.-T., 1996b. High-resolution detection of geologic boundaries from potential-field anomalies: an enhanced analytic signal technique. *Geophysics* 61, 373–386.
- Hsu, S.-K., Liu, C.-S., Thyu, C.-T., Liu, S.-Y., Sibuet, J.-C., Lallemand, S., Wang, C., Reed, D., 1998. New gravity and magnetic anomaly maps in the Taiwan-Luzon region and their preliminary interpretation. *TAO* 9 (3), 509–532.
- Hsu, S.-K., Sibuet, J.-C., Shyu, C.-T., 2001. Magnetic inversion of the East China Sea and Okinawa Trough: Tectonic implications. *Tectonophysics* 333, 111–122. [https://doi.org/10.1016/S0040-1951\(00\)00270-5](https://doi.org/10.1016/S0040-1951(00)00270-5).
- Huang, H.-H., Shyu, J.B.H., Wu, Y.-M., Chang, C.-H., Chen, Y.-G., 2012. Seismotectonics of northeastern Taiwan: kinematics of the transition from waning collision to subduction and postcollisional extension. *J. Geophys. Res.* 117, B01313. <https://doi.org/10.1029/2011JB008852>.
- Huang, P., Hsu, S.-K., Chen, S.-C., Tsai, C.-H., 2021. Flank Failure of the Volcanic Turtle Island and the Submarine Landslide in the Southernmost Okinawa Trough. Chapter 29, Book ISBN: 978-3-030-60195-9, 5 pages.
- Ichikawa, Y., 1934. 1934: Geological Map of Taiwan, TOI Sheet N°15, Scale: 1:50,000 + Explanatory Text of the Geological Map of Taiwan. Bureau of productive Industries, Government - General of Taiwan, Taihoku.
- Industrial Technology Research Institute, 2013. The Airborne Geophysical Survey of Igneous Bodies and Geological Structures in North Taiwan (2/2). Final report. Central Geological Survey (170 pp).
- Juang, W.S., Chen, J.C., 1989. Geochronology and geochemistry of volcanic rocks in northern Taiwan. *Bull. Geol. Survey* 5, 31–66.
- Kang, C.-C., Chang, C.-P., Siame, L., Lee, J.-C., 2015. Present day surface deformation and tectonic insights of the extensional Ilan Plain. *JAES* 105, 408–417.
- Kao, H., Shen, S.S.J., Ma, K.-F., 1998. Transition from oblique subduction to collision: Earthquakes in the southernmost Ryukyu arc-Taiwan region. *J. Geophys. Res.* 103, 7211–7229. <https://doi.org/10.1029/97JB03510>.
- Kimura, M., 1985. Back-arc rifting in the Okinawa trough August. *Mari. Petrol. Geol.* 2, 222–240.
- Konstantinou, K.I., Pan, C.-Y., Lin, C.-H., 2013. Microearthquake activity around Kueishantao island, offshore northeastern Taiwan: Insights into the volcano-tectonic interactions at the tip of the southern Okinawa Trough. *Tectonophysics* 593, 20–32.
- Ku, C.-Y., Hsu, S.-K., Sibuet, J.-C., Tsai, C.-H., 2009. The neotectonic structure of the southwestern tip of the Okinawa Trough. *Terrest. Atmos. Oceanic Sci.* 20, 749–759. [https://doi.org/10.3319/TAO.2008.09.01.01\(Oc\)](https://doi.org/10.3319/TAO.2008.09.01.01(Oc)).
- Kuo, F.-W., 2001. Preliminary Investigation of Shallow Hydrothermal Vents on Kueishantao Islet of Northeastern Taiwan (Master Thesis in Chinese). National Sun Yat-Sen University, Taiwan, 90p.
- Lai, K.-Y., Chen, Y.E.-G., Wu, Y.-M., Avouac, J.-P., Kuo, Y.-T., Wang, Y., Chang, C.-H., Lin, K.-C., 2009. The 2005 Ilan earthquake doublet and seismic crisis in northeastern Taiwan: evidence for dyke intrusion associated with on-land propagation of the Okinawa Trough. *Geophys. J. Int.* 179 (2), 678–686. <https://doi.org/10.1111/j.1365-246X.2009.04307.x>.
- Lallemand, S., Liu, C.-S., 1998. Geodynamic implications of present-day kinematics in the southern Ryukyus. *J. Geol. Soc. China* 41, 551–564.
- Lee, L.-L., 2005. The Study of Active Submarine Volcanoes and Hydrothermal Vents in the Southernmost Part of Okinawa Trough (Master Thesis in Chinese). National Taiwan Ocean University, Taiwan, 55p.
- Lee, J.-C., Angelier, J., Chu, H.-T., 1997. Lishan Fault... Polyphase history and kinematics of a complex major fault zone in the northern Taiwan mountain belt: the Lishan Fault. *Tectonophysics* 274, 97–115.
- Letouzey, J., Kimura, M., 1986. The Okinawa Trough: genesis of a back-arc basin developing along a continental margin. *Tectonophysics* 125, 209–230.
- Marumo, K., Hattori, K.-H., 1999. Seafloor hydrothermal clay alteration at jade in the Back-arc Okinawa Trough: Mineralogy, geochemistry and isotope characteristics. *Geochem. Cosmochim. Acta* 63 (18), 2785–2804. PII S0016-7037(99)00158-1.
- Mouyen, M., Steer, P., Chang, K.J., Le Moigne, N., Hwang, C., Hsieh, W.C., Jeandet, L., Longuevergne, L., Cheng, C.C., Boy, J.P., Masson, F., 2020. Quantifying sediment mass redistribution from joint time-lapse gravimetry and photogrammetry surveys. *Earth Surf. Dynam.* 8, 555–577. <https://doi.org/10.5194/esurf-8-555-2020>.
- Rau, R.-J., Ching, K.-E., Hu, J.-C., Lee, J.-C., 2008. Crustal deformation and block kinematics in transition from collision to subduction: Global positioning system measurements in northern Taiwan, 1995–2005. *J. Geophys. Res.* 113, B09404. <https://doi.org/10.1029/2007JB005414>.
- Shyu, J.-B.H., Sieh, K., Chen, Y.-G., Liu, C.-S., 2005. Neotectonic architecture of Taiwan and its implications for future large earthquakes. *J. Geophys. Res.* 110 (B08402), 1–33. <https://doi.org/10.1029/2004JB003251>.
- Sibuet, J.C., Letouzey, J., Barbier, F., Charvet, J., Foucher, J.-P., Hilde, T.W., Kimura, M., Chiao, L.-Y., Marsset, B., Muller, C., Stephan, J.F., 1987. Back arc extension in the Okinawa Trough. *J. Geophys. Res. Solid Earth* 92, 14041–14063. <https://doi.org/10.1029/JB092iB13p14041>.
- Sibuet, J.C., Hsu, S.K., Le Pichon, X., Le Formal, Reed, D., Moore, G., Liu, C.S., 2002. East Asia plate tectonics since 15 Ma: constraints from the Taiwan region. *Tectonophysics* 344 (1–2), 103–134.
- Sibuet, J.C., Hsu, S.-K., Shyu, C.-T., Liu, C.-S., 1995. Structural and kinematic evolutions of the Okinawa Trough backarc basin. In: *Backarc Basins*. Springer, pp. 343–379.
- Sibuet, J.-C., Deffontaines, B., Hsu, S.-K., Thureau, N., Le Formal, L., Liu, C.-S., the ACT party, 1998. Okinawa trough backarc basin: early tectonic and magmatic evolution. *J. Geophys. Res. Solid Earth* 103, 30245–30267. <https://doi.org/10.1029/98JB01823>.
- Teng, L.-S., 1996. Extensional collapse of the northern Taiwan mountain belt. *Geology* 24, 949–952.
- Tong, L.-T., Lin, W., Lee, P.-T., Lee, J.-F., Lin, C.-W., Liu, C.-Y., Chien, J.-M., Huang, Y.-T., 2013a. Airborne magnetic survey in the Kueishantao Volcano Area, Taiwan. In: *Western Pacific Sedimentology Meeting*.
- Tong, L.-T., Lin, W., Lee, P.T., Chang, S.F., Lee, J., Lee, F., 2013b. The Airborne Geophysical Survey of Igneous Bodies and Geological Structures in Northeast Taiwan Central Geological Reports. Ministry of Economic Affairs, 140pp.
- Tsai, Y.B., Feng, C.C., Chiu, J.M., Liaw, H.B., 1975. Correlation between microearthquakes and geological faults in the Hsintien-Ilan area. *Pet. Geol. Taiwan* 12, 149–167.
- Tsai, Y.B., Teng, T.-L., Chiu, J.M., Liu, H.L., 1977. Tectonic implications of the seismicity in the Taiwan region. *Mem. Geol. Soc. China* 2, 13–41.
- Tsai, Y.B., Liaw, Z.S., Lee, T.Q., Lin, M.T., Yeh, Y.H., 1981. Seismological evidence of an active plate boundary in the Taiwan area. *Mem. Geol. Soc. China* 4, 143–154.
- Tsai, C.-H., Hsu, S.-K., Chen, S.-C., Wang, S.-Y., Lin, L.-K., Huang, P.-C., Chen, K.-T., Lin, H.-S., Liang, C.-W., Cho, Y.-Y., 2021. Active tectonics and volcanism in the southernmost Okinawa Trough back-arc basin derived from deep-towed sonar surveys. *Tectonophysics* 817. <https://doi.org/10.1016/j.tecto.2021.229047>.
- Wu, F.T., Rau, R.-J., Salzberg, D., 1997. Taiwan orogeny: thin-skinned or lithospheric collision. *Tectonophysics* 274, 191–220. [https://doi.org/10.1016/S0040-1951\(96\)00304-6](https://doi.org/10.1016/S0040-1951(96)00304-6).
- Wang, K.L., Chung, S.L., Chen, C.H., Shinjo, R., Yang, T.F., Chen, C.H., 1999. Post-collisional magmatism around northern Taiwan and its relation with opening of the Okinawa Trough. *Tectonophysics* 308 (3), 363–376.
- Wu, F.-T., Liang, W.-T., Lee, J.-C., Benz, H., Villasenor, A., 2009. A model for the termination of the Ryukyu subduction zone against Taiwan: a junction of collision, subduction/separation, and subduction boundaries. *J. Geophys. Res.* 114, B07404, 1–16. <https://doi.org/10.1029/2008JB005950>.
- Yang, T.-F., Lan, T.-F., Lee, H.-F., Fu, C.-C., Chuang, P.-C., Lo, C.-H., Chen, C.-H., Chen, C.T.A., Lee, C.-S., 2005. Gas compositions and helium isotopic ratios of fluid samples around Kueishantao, NE offshore Taiwan and its tectonic implications. *Geochem. J.* Jpn. 39, 469–480.
- Yeh, Y.-H., Lin, C.-H., Roecker, S.-W., 1989. A study of upper crustal structures beneath northeastern Taiwan: possible evidence of the western extension of Okinawa Trough. *Proc. Geol. Soc. China* 16, 19–27.
- Yeh, Y.-H., Barrier, E., Lin, C.-H., Angelier, J., 1991. Stress tensor analysis in the Taiwan area from focal mechanisms of earthquakes. *Tectonophysics* 200, 267–280. [https://doi.org/10.1016/0040-1951\(91\)90019-0](https://doi.org/10.1016/0040-1951(91)90019-0).
- Yu, S.-B., Lee, C., 1986. Geodetic measurement of horizontal crustal deformation in eastern Taiwan. *Tectonophysics* 125, 73–85.
- Yu, S.-B., Tsai, Y.-B., 1979. Geomagnetic anomalies of the Ilan plain, Taiwan. *Petrol. Geol. Taiwan* 16, 19–27.
- Yu, S.-B., Chen, H.-Y., Kuo, L.-C., 1997. Velocity field of GPS stations in the Taiwan area. *Tectonophysics* 274, 41–59.
- Zeng, Z.-G., Liu, C.-H., Chen, C.-T.A., Yin, X.-B., Chen, D.-G., Wang, X.-Y., Wang, X.-M., Zhan, G.-L., 2007. Origin of a native sulfur chimney in the Kueishantao hydrothermal field, offshore Northeast Taiwan. *Sci. China Ser. D Earth Sci.* 50 (article Number 17461746-1753).